NOTICE

The quality of this microfiche is heavily dependent upon the quality of the original thesis submitted for microfilming. Every effort has been made to ensure the highest quality of reproduction possible.

If pages are missing, contact the university which granted the degree.

Some pages may have indistinct print especially if the original pages were typed with a poor typewriter ribbon or if the university sent us a poor photocopy.

Previously copyrighted materials (journal articles, published tests, etc.) are not filmed.

Reproduction in full or in part of this film is governed by the Canadian Copyright Act, R.S.C. 1970, c. C-30. Please read the authorization forms which accompany this thesis.

THIS DISSERTATION
HAS BEEN MICROFILMED
EXACTLY AS RECEIVED

AVIS

La qualité de cette microfiche dépend grandement de la qualité de la thèse soumise au microfilmage. Nous avons tout fait pour assurer une qualité supérieure de reproduction.

S'il manque des pages, veuillez communiquer avec l'université qui a conféré le grade.

La qualité d'impression de certaines pages peut laisser à désirer, surtout si les pages originales ont été dactylographiées à l'aide d'un ruban usé ou si l'université nous a fait parvenir une photocopie de mauvaise qualité.

Les documents qui font déjà l'objet d'un droit d'auteur (articles de revue, examens publiés, etc.) ne sont pas microfilmés.

La reproduction, même partielle, de ce microfilm est soumise à la Loi canadienne sur le droit d'auteur, SRC 1970, c. C-30. Veuillez prendre connaissance des formules d'autorisation qui accompagnent cette thèse.

LA THÈSE A ÉTÉ
MICROFILMÉE TELLE QUE
NOUS L'AVONS REÇUE

UNIVERSITÉ D'OTTAWA
UNIVERSITY OF OTTAWA

AN EXPERIMENTAL AND THEORETICAL STUDY OF CONVERSIONS AND TEMPERATURE RISES IN AN ADIABATIC LIQUID-FLOW TUBULAR REACTOR

by

F. Vena

A thesis submitted to the School of Graduate Studies in partial fulfillment of the requirements for the degree of M.A.Sc. in Chemical Engineering.

University of Ottawa
Ottawa, Canada, 1975

ABSTRACT

Temperature and concentration profiles in a tubular reactor in which a homogeneous irreversible first order reaction was occurring has been studied. Three flow models were investigated: i) the plug flow ii) laminar flow without radial diffusion and iii) laminar flow with radial diffusion. Basic differential equations were developed from the general equations of continuity and energy. From the basic differential equations, dimensionless expressions for the radial concentration and temperature values at any point along the reactor length were developed in which dimensionless groups of the properties of the system were introduced. The equations were solved numerically by the Crank-Nicholson finite difference technique. Experimental data was obtained for the hydration of acetic anhydride. The reactor was operated vertically under laminar flow and adiabatic conditions. Some of the main findings were:

1. For the laminar flow models:
   a) molecular diffusion had a negligible effect on the concentration and temperature profiles.
   b) the concentration profiles decreased from the center to the wall and flattened out at higher axial distances.
   and c) the temperature profiles initially exhibited a maximum at the wall which shifted towards the centre as the reaction proceeded.
2. The experimental radial temperature profiles were generally flatter than the theoretically predicted ones. Average temperatures showed better agreement at lower axial distances.

ACKNOWLEDGMENT

The author wishes to acknowledge the encouragement and guidance of Dr. J.A. Golding throughout the course of this work.

He also wishes to thank Mr. G. Casperetti for his help in constructing some of the apparatus.

Financial assistance was received through a National Research Council Grant.

TABLE OF CONTENTS

LIST OF TABLES

LIST OF FIGURES

NOMENCLATURE

Symbol	Definition
a	dimensionless radial distance, r/R_o
A_I	frequency factor (sec^{-1})
C_p	specific heat (cal)/(g - °C)
D_{AM}	diffusivity of reactant A (cm^2/sec)
E	activation energy (cal)/(g - mole)
G_1	Lewis number group, $\rho C_p D_{AM}/k_c$
G_2	activation energy group, E/RT_o
G_3	frequency factor group, $R_o^2 \rho C_p A_I/k_c$
G_4	heat of reaction group, $-\Delta H \rho A_o/\rho C_p T_o$
ΔH	heat of reaction per mole of reactant A, (cal)/(g - mole)
k_I	reaction rate constant for first-order reaction, (sec^{-1})
k_c	thermal conductivity (cal)/(cm-sec-°C)
r	radial distance (cm)
r_A	reaction rate for A (g-mole)/($sec-cm^3$)
R_o	inside tube radius (cm)
R	universal gas constant (cal)/(g-mole-°C)
S_c	rate of heat generation by chemical reaction (cal)/($sec-cm^3$)
t	time (sec)
T	absolute temperature (°K)

Symbol	Definition
T_o	inlet temperature (°K)
v	axial velocity (cm/sec)
$\langle v \rangle$	average velocity (cm/sec)
x	dimensionless concentration, ρ_A/ρ_{A_o}
w	dimensionless axial distance, $(k_c Z)/(2 R_o^2 \langle v \rangle \rho C_p)$
Z	axial distance (cm)
ρ	density of reacting mixture (g/cm^3)
ρ_A	concentration of reactant A (g-mole)/(cm^3)
ρ_{A_o}	inlet concentration of reactant A (g-mole)/(cm^3)
θ	dimensionless temperature $(T - T_o)/T_o$
μ	viscosity of reacting mixture
$\langle x \rangle$	average dimensionless concentration
$\langle \theta \rangle$	average dimensionless temperature

Finite Difference Terms

Symbol	Definition
h	radial incremental spacing
k	axial incremental spacing
m	radial position (level)
n	axial position (level
s	wall position

Subscripts

Symbol	Definition
Á	reactant A
m	radial position
n	axial position
o	inlet condition
s	wall value

I - INTRODUCTION

The problem of predicting conversions in laminar flow tubular reactors has recently attracted considerable attention. In this type of reactor, the parabolic velocity profile leads to a distribution of contact times which gives rise to radial concentration gradients which in turn induce radial diffusion. In non-isothermal systems the situation is even more complex due to radial temperature gradients which cause a variation of reaction rate which also influences the concentration gradients.

The analysis of an isothermal viscous flow reactor has been carried out by Cleland and Wilhem[1]. They solved the equation of species continuity for a homogeneous first-order reaction by the finite difference method, assuming constant physical properties and fully developed laminar flow. They showed the effect of radial diffusion on reaction conversion and supported their theoretical solution with experimental data. Vignes and Trambouzie[2] extended the analysis of Cleland and Wilhelm to a second-order homogeneous reaction.

Non-isothermal systems in which the basic differential equations were developed from the general equations of continuity, motion and energy[9] and solved numerically have also been studied. Rothenberg and Smith[7,8] studied the effect of reaction and heat transfer in laminar tube flow. They gave particular attention to the effect reaction and diffusion had on the heat transfer characteristics of the reactor. They predicted concentration and temperature profiles as well as average cup-mixing concentrations and temperatures and also investigated the effect of system parameters. Andersen and Coull[14] using a finite difference method similar to that of Rothenberg and Smith, took into account the temperature dependence of diffusivity and concluded that this had a negligible effect. More industrially-oriented systems were investigated by Trombetta and

Happel[13] and Merrill and Hamrin[10]. Trombetta and Happel studied the analysis and design of gas flow reactors with applications to hydrocarbon pyrolysis. They presented their results as factors which can be used to correct calculations with the plug flow assumption. Merrill and Hamrin investigated the demethylation of toluene in the presence of hydrogen under isothermal, constant wall temperature, and adiabatic reaction conditions. They presented their results in the form of conversion and temperature profiles.

The present investigation is an attempt to analyse the problem of predicting concentration and temperature profiles in tubular reactors using the Crank-Nicholson finite difference technique. Three models will be studied:

a) plug flow

b) laminar flow without radial diffusion

c) laminar flow with radial diffusion

under adiabatic reactor conditions. The hydration of acetic anhydride, a pseudo-first order reaction with well know kinetics[1,25,26] in dilute solution, is the reaction investigated.

II - LITERATURE SURVEY

Considerable interest has recently been shown in laminar flow tabular reactors[1-6]. The problem of predicting overall conversion as well as radial concentration and temperature gradients has received the greatest attention. It was generally found that the velocity profile, the temperature profile and axial mixing affected conversion.

Cleland and Wilhelm[1] studied the effect on point and integral average conversion of a chemical reaction, coupled with radial diffusion and radial distribution of reaction times in a viscous-flow tubular reactor. The investigation was limited to an analysis of a reaction occurring isothermally in laminar flow, therefore only mass transfer equations were considered. Approximate solutions were obtained by numerical integration of the corresponding finite difference equations. The derived equations for reaction, flow, and diffusion formed a proper description of the experimental results as applied to the hydrolysis of acetic anhydride.

It was concluded that axial diffusion can be safely neglected but that radial diffusion can only be neglected when:

$$\frac{D_{AM} L}{u_o R_o^2} < 1.95 \times 10^{-3} \qquad (I)$$

where D_{AM} is the diffusion coefficient
L is the reactor length
u_o is the centre line velocity
R_o is the tube radius

However it was found that under certain conditions free convection, which was not included through terms in the original rate equation, may be

important in laminar flow tubular reactors. The free convective process becomes established when the density gradient in the system exceeds a certain value. The density gradient may be due to a temperature gradient, a concentration gradient, or a combination of the two. The convective processes cause mass and heat transfer rates within a fluid layer to be increased so that, in effect, conductivities and diffusivities are increased. Cleland and Wilhelm noted that the value of D_{AM} in equation (I) could be considerably different than the molecular diffusivity when free convection effects were prominent. Vignes and Trambouzie[2] came to similar conclusions and extended their analysis to a second order reaction.

Chambré[3] established a general analytical method for the prediction of specie concentration changes and temperature rises for mildly non-isothermal systems. For a system with a fully established velocity field, the specie concentration can be found from a single function i. e. the degree of advancement of the reaction, while the temperature is determined through a generalized enthalpy function which takes into account the thermal exchange with the exterior.

Rothenberg and Smith[7, 8] made an analytical study on the effect of velocity profile, reaction conditions and reaction kinetics on concentration and temperature profiles in a tubular reactor under laminar flow. They studied a gas phase first-order homogeneous irreversible reaction. The basic differential equations were developed from the general equations of continuity, motion and energy as described in Bird, Stewart and Lightfoot[9].

From the basic differential equations, dimensionless expressions for the radial composition and temperature values at any point along the reactor length were developed. The solutions for these expressions were obtained using finite difference techniques by machine computation.

The results obtained showed the effect of the G parameters (see theoretical discussion) on point and bulk reactant concentration and temperature profiles. The following discussion will be limited to the results obtained for an exothermic reaction with constant wall temperature. The parameters G_1, G_2, G_3, and G_4 were chosen to represent typical gaseous reactions.

The most significant factor was the heat of reaction group G_4. For bulk temperature, it was noted that the distance of the maximum temperature from the reactor inlet first increased and then decreased as the heat of reaction was increased. The peak became sharper as G_4 values were increased. Rothenberg reported that the solution became unstable for G_4 values greater than 0.370. For bulk composition, the reactant decreased more rapidly, the higher the heat of reaction.

The radial temperature and composition profiles showed changing trends. The composition profiles at low axial distances decreased from the center to the wall. This was due to the fact that initially, the temperature at the centre was not much greater than that at the wall. Therefore, the increased rate of reaction at the centre was more than balanced by the longer reaction time near the wall and more reactant was consumed at the latter location. This effect became more pronounced as the heat of reaction decreased. At higher axial distances, a reversal in trend was noticed. Here, the higher temperatures at the centre of the reactor increased the reaction rate which more than offset the increased residence time at the wall. Therefore the concentration was much lower at the centre than at the wall.

Similarly the radial temperature profiles exhibited a changing behaviour at different axial distances. The temperature near the centre rose initially to a maximum as the axial distance increased and then reversed its trend and decreased with increasing axial distance.

The previous results were all restricted to a Lewis number typical of gases. For liquids, a much smaller value would be more appropriate. Here the diffusivity was much less, and the system would behave somewhat like annular layers of fluid which were separated by impermeable membranes. The chief effect of changes in the Lewis number was on the radial profiles. As would be expected, the composition gradients were large and the reactant concentration was lower at the wall than at the centre. Again the reduction near the wall was caused by the longer residence time.

Merrill and Hamrin[10] investigated the mass and heat transfer equations describing radial and axial profiles for tubular reactors for the exothermic vapour phase demethylation of toluene in the presence of hydrogen. No experimental results were given but analytical solutions for isothermal, constant wall temperature, and adiabatic reactor conditions were described. Both diffusion and-non diffusion were considered.

The basic differential equations were again developed from the general equations of continuity, motion, and energy and solved by finite-difference techniques by using a computer. Conversion of the partial differential equations to finite-difference equations was carried out by the method outlined by Jensen and Jeffreys[11]. Radial conversion and temperature profiles were obtained as a function of reactor length and volume in dimensionless forms. Only the results obtained under laminar flow will be discussed here.

For the isothermal reactor, the conversion was shown to remain relatively constant over half of the tube radius and then to increase sharply to the wall conversion. The constant wall temperature reactor showed the same constant behaviour for low axial distances. As the axial distance along the reactor increased, the effect of the exothermic nature of the reaction on conversion became readily apparent. For the

maximum reactor length, the centre live conversion for this reaction was 0.68, whereas for the isothermal reactor it was only 0.32. The adiabatic and constant wall temperature profiles are superimposable over half of the tube radius. Beyond this, the adiabatic conversion was higher as the wall was approached.

The effect of neglecting radial diffusion was found to be most significant for the isothermal case near the wall. Conversion at the wall with diffusion was 0.74; neglecting diffusion gave a value of 1.0. Only slight differences over the entire reactor radius were evident for the constant wall temperature and adiabatic cases. The flow average conversions at the maximum reactor length showed that the effect of neglecting diffusion in all three cases, amounts to less than 5% difference on the overall conversion.

These results were in agreement with the criterion suggested by Bosworth [12] for determining the importance of diffusion. He defined as dimensionless number $D_{AM} L / U_o R_o^2$ (see equation I) and stated that when this number was less than 3.1×10^{-3} diffusion was negligible. Cleland and Wilhelm as described earlier, obtained a value of 1.95×10^{-3}. This number averaged to about 3.5×10^{-3} in this study.

For the constant wall temperature reactor, it was apparent that a maximum in temperature occured which moved fromthe region near the wall at low axial distances and tended toward the center of the reactor at higher axial distances. This behaviour was due to the higher conversions of the slower moving fluid in the vicinity of the wall and the exothermic nature of the reaction. Eventually this maximum would occur at the centre line as complete conversion was achieved. In the adiabatic reactor a sharp temperature rise was observed near the wall a low axial distances. This temperature increase became less pronounced for higher axial distances. This trend showed that the reactor was approaching

the upper limit for total conversion.

Overall conversions were also compared for similar conditions in laminar and plug flow reactors of the same volume. It was interesting to note than an isothermal, laminar flow reactor of a given volume gave about the same conversion as an isothermal plug flow reactor of the same volume. This was also true for the adiabatic reactors up to a conversion of 0.4, after which the conversion in the plug flow case increased faster than the laminar. For the constant wall temperature reactors, the conversions varied considerably, approaching adiabatic conversion for laminar flow and isothermal conversion for plug flow.

It was thus concluded that an adiabatic reactor operating with plug flow appeared most desirable for the demethylation of toluene. Second choice would be adiabatic or constant wall temperature in laminar flow. This was followed by isothermal or constant wall temperature in plug flow. Least desirable was an isothermal plug flow reactor.

Trombetta and Happel[13] adapted a different approach to study the effect of radial concentration and temperature gradients in a first-order reaction in a compressible fluid under laminar flow. They were particularly interested in hydrocarbon pyrolysis systems. The same basic equations were used of continuity, motion, and energy. The Arrhenius dependence of reaction rate on temperature was assumed. Dimensionless equations were formulated and their method of solution consisted in deriving integral forms of the above basic equations by writing macroscopic balances across disk dements. Ordinary differential equations were then developed for the dependent variables in even power series in the independent variable. By substituting the differential equations into the integral equations, simultaneous ordinary differential equations were thus derived. The Gaussian elimination technique was used to solve the set of equations at each axial position and the Runge -Kutta method was

then applied to integrate axially. By this method, they were able to follow the progress of the reaction and at suitable intervals, calculate average reactant concentration and the average temperature.

They were thus able to compare their results to solutions based on the plug flow model and draw a set of graphs giving correction factors to be applied to plug flow kinetic constants and reactor lengths in the analysis and design of gas flow reactors. They found that the effects of temperature gradients were far more important than the effects of concentration and that correction factors of two, three and even higher were not uncommon. It was also noted that distortions of the parabolic velocity profile had a minor effect on the correction factor.

Andersen and Coull[14] compared the approach of Rothenberg and Smith with that of Trombetta and Happel to the analysis of a tubular laminar flow gas-phase reactor. They followed the solution of the type presented by Rothenberg and Smith and extended it to accomodate it to changes in the total number of moles (e.g. concentrated and dilute feed conditions) and also to a reactor operating adiabatically. Their results agreed most favourably with those of Rothenberg and Smith, and Trombetta and Happel.

III - THEORETICAL

The differential equations used for developing the concentration and temperature profiles are the equations of continuity and energy as given in Bird, Stewart, and Lightfoot[9]. Assuming ρ, μ, k, and D_{AM} to be constant, the following equations arise.

Continuity Equation:

$$\frac{D\rho_A}{Dt} = D_{AM} \nabla^2 \rho_A + r_A \qquad (1)$$

Energy Equation:

$$\rho C_p \frac{DT}{Dt} = k_c \nabla^2 T + S_c \qquad (2)$$

Other simplifying assumptions used in developing the final equations are:

(1) the reaction rate constant can be described by the Arrhenius equation for a first order reaction

$$r_A = -k_I \rho_A = -A_I \rho_A \exp\left(\frac{-E}{RT}\right) \qquad (3)$$

(2) the heat of reaction ΔH is constant over the reactor length

(3) the velocity profiles are fully developed; that is for plug flow

$$v = \langle v \rangle \qquad (4)$$

and for laminar flow

$$v = 2\langle v\rangle \left[1 - (r/R_o)^2\right] \tag{5}$$

(4) axial mass and energy transport due to diffusion and conduction are negligible compared to convective transport

(5) steady state

A. Differential Equations:

The differential equations of continuity and energy developed from equations (1) and (2) under the assumptions made follow:

Case 1 (Plug Flow)

Continuity Equation

$$\langle v\rangle \frac{d\rho_A}{dz} + A_I \rho_A \exp\left(\frac{-E}{RT}\right) = 0 \tag{6}$$

Energy Equation

$$\langle v\rangle \frac{\partial T}{\partial z} = \frac{\Delta H \rho_A}{\rho C_p} A_I \exp\left(\frac{-E}{RT}\right) \tag{7}$$

Case 2 (Laminar Flow without Radial Diffusion)

Continuity Equation

$$2\langle v\rangle \left[1 - (r/R_o)^2\right] \frac{\partial \rho_A}{\partial z} + A_I \rho_A \exp\left(\frac{-E}{RT}\right) = 0 \tag{8}$$

Energy Equation

$$2\langle v\rangle \left[1-(r/R_o)^2\right]\frac{\partial T}{\partial z}=\frac{k_c}{\rho C_p}\left(\frac{1}{r}\frac{\partial T}{\partial r}+\frac{\partial^2 T}{\partial r^2}\right)+$$

$$\frac{\Delta H \rho_A}{\rho C_p} A_I \exp\left(\frac{-E}{RT}\right) \qquad (9)$$

Case 3 (Laminar Flow with Radial Diffusion)

Continuity Equation

$$2\langle v\rangle \left[1-(r/R_o)^2\right]\frac{\partial \rho_A}{\partial z}=D_{AM}\left(\frac{1}{r}\frac{\partial \rho_A}{\partial r}+\frac{\partial^2 \rho_A}{\partial r^2}\right)$$

$$-A_I \rho_A \exp\left(\frac{-E}{RT}\right) \qquad (10)$$

Energy Equation

$$2\langle v\rangle \left[1-(r/R_o)^2\right]\frac{\partial T}{\partial z}=\frac{k_c}{\rho C_p}\left(\frac{1}{r}\frac{\partial T}{\partial r}+\frac{\partial^2 T}{\partial r^2}\right)+$$

$$\frac{\Delta H \rho_A}{\rho C_p} A_I \exp\left(\frac{-E}{RT}\right) \qquad (11)$$

Equations (6) to (11) are subsequently transformed into dimensionless form and the groups and variables chosen are:

G_1, Lewis number group $= \rho C_p D_{AM}/k_c$ (12)

G_2, activation energy group $= E/RT_o$ (13)

G_3, frequency factor group $= R_o^2 \rho C_p A_I / k_c$ (14)

G_4, heat of reaction group $= -\Delta H \rho_{A_o} / \rho C_p T_o$ (15)

$a = r/R_o$ (16)

$x = \rho_A / \rho_{A_o}$ (17)

$w = k_c Z / (2 R_o^2 \langle v \rangle C_p \rho)$ (18)

$\theta = (T - T_o)/T_o$ (19)

The corresponding equations in dimensionless form follow:

Case 1 (Plug Flow)

Continuity Equation

$$\frac{dx}{dw} + 2 x G_3 \exp\left(\frac{-G_2}{\theta + 1}\right) = 0 \qquad (20)$$

Energy Equation

$$\frac{\partial \theta}{\partial w} = 2 x G_3 G_4 \exp\left(\frac{-G_2}{\theta + 1}\right) \qquad (21)$$

Case 2 (Laminar Flow-without Radial Diffusion)

Continuity Equation

$$\frac{dx}{dw} + \frac{x G_3}{(1 - a^2)} \cdot \exp\left(\frac{-G_2}{\theta+1}\right) = 0 \qquad (22)$$

Energy Equation

$$\frac{\partial \theta}{\partial w} = \frac{1}{(1 - a^2)} \left(\frac{1}{a} \frac{\partial \theta}{\partial a} + \frac{\partial^2 \theta}{\partial a^2} \right) + \frac{x G_3 G_4}{(1 - a^2)} \exp \left(\frac{-G_2}{\theta + 1} \right) \quad (23)$$

Case 3 (Laminar Flow-With Radial Diffusion)

Continuity Equation

$$\frac{\partial x}{\partial w} = \frac{G_1}{(1 - a^2)} \left(\frac{1}{a} \frac{\partial x}{\partial a} + \frac{\partial^2 x}{\partial a^2} \right) - \frac{x G_3}{(1 - a^2)} \exp \left(\frac{-G_2}{\theta + 1} \right) \quad (24)$$

Energy Equation

$$\frac{\partial \theta}{\partial w} = \frac{1}{(1 - a^2)} \left(\frac{1}{a} \frac{\partial \theta}{\partial a} + \frac{\partial^2 \theta}{\partial a^2} \right) + \frac{x G_3 G_4}{(1 - a^2)} \exp \left(\frac{-G_2}{\theta + 1} \right) \quad (25)$$

The boundary conditions for the adiabatic reactor at the wall are summarized below:

FLOW MODEL	ADIABATIC REACTOR CONDITIONS AT WALL; a = 1	
Plug Flow	$\frac{\partial \theta}{\partial a} = 0$	(26)

Laminar Flow Without Radial Diffusion

$$x = 0 \tag{27}$$

$$\frac{\partial \theta}{\partial a} = 0. \tag{28}$$

Laminar Flow with Radial Diffusion

$$\frac{\partial x}{\partial a} = 0 \tag{29}$$

$$\frac{\partial \theta}{\partial a} = 0 \tag{30}$$

At the centre line, the following conditions are imposed from the assumption of symmetry:

$$\frac{\partial \theta}{\partial a} = 0 \tag{31}$$

$$\frac{\partial x}{\partial a} = 0 \tag{32}$$

B. Numerical Procedure:

The equations to be solved are parabolic[15] and the Crank-Nicholson type finite difference method as suggested by Lapidus[15] is used. In this method, the derivatives for x are approximated by:

$$\frac{\partial x}{\partial w} \left(x_{m,n+1} - x_{m,n} \right) / k \tag{33}$$

$$\frac{\partial x}{\partial a} = \frac{1}{4h} \left[\left(\theta_{m+1,n+1} - \theta_{m-1,n+1} \right) + \left(\theta_{m+1,n} - \theta_{m-1,n} \right) \right] \tag{34}$$

and $$\frac{\partial^2 x}{\partial a^2} = \frac{1}{2h^2}\left[\left(\theta_{m+1,n} - \partial\theta_{m,n+1} + \theta_{m-1,n+1}\right) + \left(\theta_{m+1,n} - \partial\theta_{m,n} + \theta_{m-1,n}\right)\right] \quad (35)$$

where x is defined as

$$x = \left(x_{m,n+1} + x_{m,n}\right)/2 \quad (36)$$

Analogous expressions are used for θ.

From the finite difference equations, two sets of linear simultaneous equations were derived and were solved alternately on an IBM 360/65 computer. The concentration change was calculated first, and the corresponding temperature rise evaluated. The temperature rise was required before the next concentration change could be calculated. This procedure was repeated along the whole length of the reactor. A standard Gaus-Jordan elimination subroutine was employed in determining the temperature profiles and for the third flow model.

The development of the simultaneous linear equations for the three flow models follows. The subscripts S and S-1 denote the grid points at the wall and one step away from the wall respectively. The axial position at n=1 represents the inlet to the reactor.

Case 1 (Plug Flow)

The equation of continuity in dimensionless form is given by (20)

$$\frac{dx}{dw} + 2x\, G_3 \exp\left(\frac{-G_2}{\theta+1}\right) = 0 .$$

If k is chosen sufficiently small such that the difference between $\exp\left(\frac{-G_2}{\theta_{m,n+1}+1}\right)$ and $\exp\left(\frac{-G_2}{\theta_{m,n}+1}\right)$ is negligible, then substituting equation (36) and the finite difference approximation of the derivative into (20) gives

$$x_{m,n+1} - x_{m,n} + k\,G_3\left(x_{m,n+1} + x_{m,n}\right)\exp\left(\frac{-G_2}{\theta_{m,n}+1}\right) = 0. \tag{37}$$

Collecting like terms

$$A_1 x_{m,n+1} = A_2 x_{m,n} \tag{38}$$

$$m = 1, 2, \ldots, s$$

where $A_1 = 1 + k\,G_3 \exp\left(\frac{-G_2}{\theta_{m,n}+1}\right)$ (39)

and $A_2 = 1 - k\,G_3 \exp\left(\frac{-G_2}{\theta_{m,n}+1}\right)$. (40)

The temperature profile is calculated from the energy equation (21)

$$\frac{\partial\theta}{\partial w} = 2\,x\,G_3\,G_4 \exp\left(\frac{-G_2}{\theta+1}\right)$$

which in finite difference form, becomes

$$A_4\,\theta_{m,n+1} + A_5\,\theta_{m,n} + A_5 \qquad (41)$$

$$m = 1, 2, \ldots, S.$$

Where

$$A_3 = 1 \qquad (42)$$

$$A_4 = 1 \qquad (43)$$

and

$$A_5 = k\,G_3\,G_4\left(x_{m,n+1} + x_{m,n}\right)\exp\left(\frac{-G_2}{\theta_{m,n}+1}\right) \qquad (44)$$

Case 2 (Laminar Flow - Without Radial Diffusion)

The equation of continuity in dimensionless form is given by (22)

$$\frac{dx}{dw} + \frac{x\ G_3}{(1 - a^2)} \exp\left(\frac{-G_2}{\theta + 1}\right) = 0$$

which in finite difference form is

$$B_1 x_{m,n+1} - B_2 x_{m,n} \qquad (45)$$

$$m = 1, 2, \ldots, s-1$$

where

$$B_1 = 1 + \left[k\ G_3 \exp\left(\frac{-G_2}{\theta_{m,n} + 1}\right) / 2\left(1 - a_m^2\right) \right] \qquad (46)$$

and

$$B_2 = 1 - \left[k\ G_3 \exp\left(\frac{-G_2}{\theta_{m,n} + 1}\right) / 2\left(1 - a_m^2\right) \right] \qquad (47)$$

At the centre equation (45) is readily solvable when a=0. At the wall, ie a=1, the residence time is infinite and the concentration can be taken to be zero. Therefore

$$x_{s,n} = 0 \quad \text{for all } n>1 \ . \qquad (48)$$

The energy equation is given by (23)

$$\frac{\partial \theta}{\partial w} = \frac{1}{(1 - a^2)} \left(\frac{1}{a} \frac{\partial \theta}{\partial a} + \frac{\partial^2 \theta}{\partial a^2} \right) + x \frac{G_3\ G_4}{(1 - a^2)} \exp\left(\frac{-G_2}{\theta + 1}\right)$$

The corresponding finite difference equation becomes

$$B_3 \theta_{m+1, n+1} + B_4 \theta_{m, n+1} + B_5 \theta_{m-1, n+1} = B_6 \qquad (49)$$

$$m = 2, 3, \ldots, s-1$$

where

$$B_3 = -\left[k (h + 2a_m) / 4 (1 - a_m^2) a_m h^2 \right] \qquad (50)$$

$$B_4 = 1 + \left[k/(1 - a_m^2) h^2 \right] \qquad (51)$$

$$B_5 = \left[k (h - 2a_m) / 4 (1 - a_m^2) a_m h^2 \right] \qquad (52)$$

and

$$B_6 = \left[k (h + 2a_m) / 4 (1 - a_m^2) a_m h^2 \right] \theta_{m+1, n}$$

$$+ \left[1 - \left(k / (1 - a_m^2) h^2 \right) \right] \theta_{m, n} + \left[k \left(2a_m - h \right) \right.$$

$$\left. / 4 (1 - a_m^2) a_m h^2 \right] \theta_{m-1, n} + \frac{k G_3 G_4}{2 (1 - a_m^2)}$$

$$\left(x_{m, n+1} + x_{m, n} \right) \exp \left(\frac{-G_2}{\theta_{m, n} + 1} \right) . \qquad (53)$$

At the centre line, radial symmetry is assumed and on applying l'Hôpital's rule equation (23) becomes

$$\frac{\partial \theta}{\partial w} = 2 \frac{\partial^2 \theta}{\partial a^2} + x G_3 G_4 \exp \left(\frac{-G_2}{\theta + 1} \right) \qquad (54)$$

and the corresponding finite difference equation is

$$B_7\,\theta_{2,n+1} + B_8\,\theta_{1,n+1} = B_9 \tag{55}$$

where

$$B_7 = -2k/h^2 \tag{56}$$

$$B_8 = 1 + 2\,k/h^2 \tag{57}$$

and

$$B_9 = (2k/h^2)\,\theta_{2,n} + (1 - 2k/h^2)\,\theta_{1,n} + \frac{1}{2}\,k\,G_3\,G_4 \left(x_{1,n+1} + x_{1,n}\right) \exp\left(\frac{-G_2}{\theta_{1,n}+1}\right). \tag{58}$$

At the wall, equation (23) reduces to

$$\frac{\partial^2 \theta}{\partial a^2} + x\,G_3\,G_4 \exp\left(\frac{-G_2}{\theta+1}\right) = 0 \tag{59}$$

To simplify computation for the wall temperature, explicity formulation as suggested by hapidus[15] is adopted

$$\frac{\partial^2 \theta}{\partial a^2} = \left(\theta_{s+1,n+1} - 2\,\theta_{s,n+1} + \theta_{s-1,n+1}\right)/h^2. \tag{60}$$

For the condition $\left(\frac{\partial \theta}{\partial a}\right)_{a=1} = 0$, we have wall symmetry, that is

$$\theta_{s+1,\,n+1} = \theta_{s-1,\,n+1} \tag{61}$$

and equation (73) becomes

$$\frac{\partial^2 \theta}{\partial a^2} = \frac{2}{h^2}\left(\theta_{s-1,\,n+1} - \theta_{s,\,n+1}\right). \tag{62}$$

Substituting into equation (72) gives

$$\theta_{s,\,n+1} = \theta_{s-1,\,n+1} + \frac{h^2}{2} x_{s,\,n+1} G_3 G_4 \exp\left(\frac{-G_2}{\theta_{s,\,n+1}}\right). \tag{63}$$

However for n=1, $x_{s,\,n+1} = 0$ by definition, such that equation (76) reduces to

$$\theta_{s,\,n+1} = \theta_{s-1,\,n+1} \tag{64}$$

This is too inaccurate initially, as it ignores initial heat generation at the wall.

Using the second difference formula

$$\frac{\partial^2 \theta}{\partial a^2} = \left(-\theta_{s+2,\,n+1} + 16\,\theta_{s+1,\,n+1} - 30\,\theta_{s,\,n+1} + 16\,\theta_{s-1,\,n+1} - \theta_{s-2,\,n+1}\right) / 12h^2 \tag{65}$$

which due to wall symmetry becomes

$$\frac{\partial^2 \theta}{\partial a^2} = \left(16\, \theta_{s-1,n+1} - \theta_{s-2,n+1} - 15\, \theta_{s,n+1} \right) / 6h^2 \qquad (66)$$

and substituting into equation (59) gives

$$15\, \theta_{s,n+1} - 16\, \theta_{s-1,n+1} + \theta_{s-2,n+1} = 6h^2\, x_{s,n}\, G_3\, G_4 \exp\left(\frac{-G_2}{\theta_{s,n+1}} \right) \qquad (67)$$

Therefore, for n=1, we have

$$\theta_{s,2} - \frac{16}{15}\, \theta_{s-1,2} + \frac{1}{15}\, \theta_{s-2,2} = \frac{2}{5}\, h^2\, x_{s,1}\, G_3\, G_4 \exp\left(\frac{-G_2}{\theta_{s,1+1}} \right) \qquad (68)$$

and for $n \geq 2$

$$-\theta_{s,n+1} - \frac{16}{15}\, \theta_{s-1,n+1} + \frac{1}{15}\, \theta_{s-2,n+1} = 0 \qquad (69)$$

since by definition, $x_s = 0$ for $n > 1$.

Case 3 (Laminar Flow-with Radial Diffusion)

The equation of continuity in dimensionless form is given by (24)

$$\frac{\partial x}{\partial w} = \frac{G_1}{(1 - a^2)} \left(\frac{1}{a} \frac{\partial x}{\partial a} + \frac{\partial^2 x}{\partial a^2} \right) - \frac{x\, G_3}{(1 - a^2)} \exp\left(\frac{-G_2}{\theta + 1} \right)$$

which in finite difference form becomes

$$C_1 x_{m+1,n+1} + C_2 x_{m,n+1} + C_3 x_{m-1,n+1} = C_4 \qquad (70)$$

$$m = 2, 3, \ldots, s-1$$

where

$$C_1 = 1 k G_1 (h + 2a_m) / 4 (1 - a_m^2) a_m h^2 \qquad (71)$$

$$C_2 = 1 + \{ k G_1 / (1 - a_m^2) h^2 \} + \{ k G_3 \exp \left(\frac{-G_2}{\theta + 1} \right) / 2 (1 - a_m^2) \} \qquad (72)$$

$$C_3 = k G_1 (h - 2 a_m) / 4 (1 - a_m^2) a_m h^2 \qquad (73)$$

and

$$C_4 = \left[k G_1 (h + 2a_m) / 4 (1 - a_m^2) a_m h^2 \right] x_{m+1,n} + \left[1 - \{ k G_1 / (1 - a_m^2) h^2 \} - \{ k G_3 \exp \left(\frac{-G_2}{\theta + 1} \right) / 2 (1 - a_m^2) \} \right] x_{m,n} + \left[k G_1 (2 a_m - h) / 4 (1 - a_m^2) a_m h^2 \right] x_{m-1,n} \qquad (74)$$

At the centre line, assuming radial symmetry equation (24) becomes

$$\frac{\partial x}{\partial w} = 2 G_1 \frac{\partial^2 x}{\partial a^2} - x G_3 \exp\left(\frac{-G_2}{\theta+1}\right) \tag{75}$$

which reduces to

$$C_5 x_{2,n+1} + C_6 x_{1,n+1} = C_7 \tag{76}$$

where

$$C_5 = -2 k G_1/h^2 \tag{77}$$

$$C_6 = 1 + (2k G_1/h^2) + \frac{k G_3}{2} \exp\left(\frac{-G_2}{\theta_{1,n}+1}\right) \tag{78}$$

and

$$C_7 = (2 kG_1/h^2) x_{2,n} + \left[1 - (2 k G_1/h^2) - \frac{kG_3}{2} \exp\left(\frac{-G_2}{\theta_{1,n}+1}\right)\right] x_{1,n} \tag{79}$$

At the wall, there is no transport of material through the solid boundary and equation (24) becomes

$$G_1 \frac{\partial^2 x}{\partial a^2} - x G_3 \exp\left(\frac{-G_2}{\theta+1}\right) = 0 \tag{80}$$

Here Lapidus[15] again suggests the use of the explicit form of the finite difference equation, that is

$$\frac{\partial^2 x}{\partial a^2} = \left(x_{s+1,n+1} - 2 x_{s,n+1} + x_{s-1,n+1}\right)/h^2 \tag{81}$$

and noting that for $\left(\frac{\partial x}{\partial a}\right)_{a=1} = 0$, we have symmetry,

$$x_{s+1, n+1} = x_{s-1, n+1} \tag{82}$$

such that the concentration at the wall is given by $x_{s, n+1}$ and on substitution:

$$C_8 x_{s, n+1} + C_9 x_{s-1, n+1} = 0 \tag{83}$$

where

$$C_8 = \frac{2 G_1}{h^2} + G_3 \exp\left(\frac{-G_2}{\theta_{s, n+1}}\right) \tag{84}$$

and

$$C_9 = -2 G_1/h^2 \tag{85}$$

The energy equation is identical to that of case II and the same linear equations are obtained for the internal radial positions ($m = 2, \ldots, s-1$

At the centre line, assuming radial symmetry, equation (25) becomes

$$\frac{\partial \theta}{\partial w} = 2 \frac{\partial^2 \theta}{\partial a^2} + x G_3 G_4 \exp\left(\frac{-G_2}{\theta + 1}\right) \tag{86}$$

and the resultant finite difference equation is

$$C_{10}\,\theta_{2,n+1} + C_{11}\,\theta_{1,n+1} = C_{12} \tag{87}$$

where

$$C_{10} = -2k/h^2 \tag{88}$$

$$C_{11} = 1 + (2\,k/h^2) \tag{89}$$

and

$$C_{12} = (2\,k/h^2)\,\theta_{2,n} + \left[1 - (2\,k/h^2)\right]\theta_{1,n} + \frac{k}{2}\,(x_{1,n+1} + x_{1,n})\,G_3\,G_4\,\exp\left(\frac{-G_2}{\theta_{1,n+1}}\right) \tag{90}$$

At the wall, the equation is also identical to that of case II, and following a similar procedure gives

$$\theta_{s,n+1} - \frac{16}{15}\,\theta_{s-1,n+1} + \frac{1}{15}\,\theta_{s-2,n} = \frac{2}{5}\,h^2\,x_{s,n+1}\,G_3\,G_4\,\exp\left(\frac{-G_2}{\theta_{s,n+1}}\right) \tag{91}$$

C. Average Values

The average values for temperature and concentration at any axial position are calculated from:

Case I (Plug Flow)

$$\langle x \rangle = 2 \int_0^1 x\, a\, d\, a \tag{92}$$

$$\langle \theta \rangle = 2 \int_0^1 x\, a\, d\, a \tag{93}$$

Case II and III (Laminar Flow)

$$\langle x \rangle = 4 \int_0^1 x\,(1 - a^2)\, a\, d\, a \tag{94}$$

$$\langle \theta \rangle = 4 \int_0^1 \theta\,(1 - a^2)\, a\, d\, a\,. \tag{95}$$

These are the so called cup-mixing average values. The integrals are evaluated numerically by the use of Simpson's Rule.

IV - EXPERIMENTAL

A. Reaction

The hydration of acetic anhydride in dilute solution was chosen for this study:

$$(CH_3\,CO)_2\,O + H_2O = 2\,CH_3\,COOH$$

It is a well studied pseudo first-order reaction and its rate constants have been reported in the litterature[1,24,25]. From the data reported a least-squares fit of the Arrhenius equation as described in Appendix B gives

$$\ln k = \frac{5,352.9}{T} + 15.946$$

the heat of reaction at 20°C is -13,100 cal/mole as determined from heats of formation[26].

B. Apparatus

A schematic of the apparatus is shown in fig. I with full equipment details given in Appendix D. The apparatus was basically made up of a vertical plexiglass reactor of the following dimensions:

I.D. (cm)	Length (cm)
3.49	221

It was fitted with a 28 cm. long inlet conical section such that a smooth transition took place from the 0.48 cm. conical section inlet to the 3.49 cm outlet. The cone angle was approximately 6° to avoid boundary layer

Equipment List (See figure I)

1. Compressed air cylinder
2. Air regulator
3. Off-on valve
4. Pressure gauge
5. Off-on valve
6. Off-on valve
7. Off-on valve
8. Water side surge tank
9. Acetic anhydride surge tank
10. Needle-valve
11. Needle-valve
12. Constant temperature bath
13. Needle valve
14. Magnetic mixing chamber
15. Off-on valve
16. Off-on valve
17. Conical inlet section to reactor
18. Plexiglass reactor
19. Plexiglass reactor jacket
20. Valve
21. Valve
22. Thermocouples (TC1, TC2, TC3, TC4)
23. Acetic anhydride pump
24. Water pump

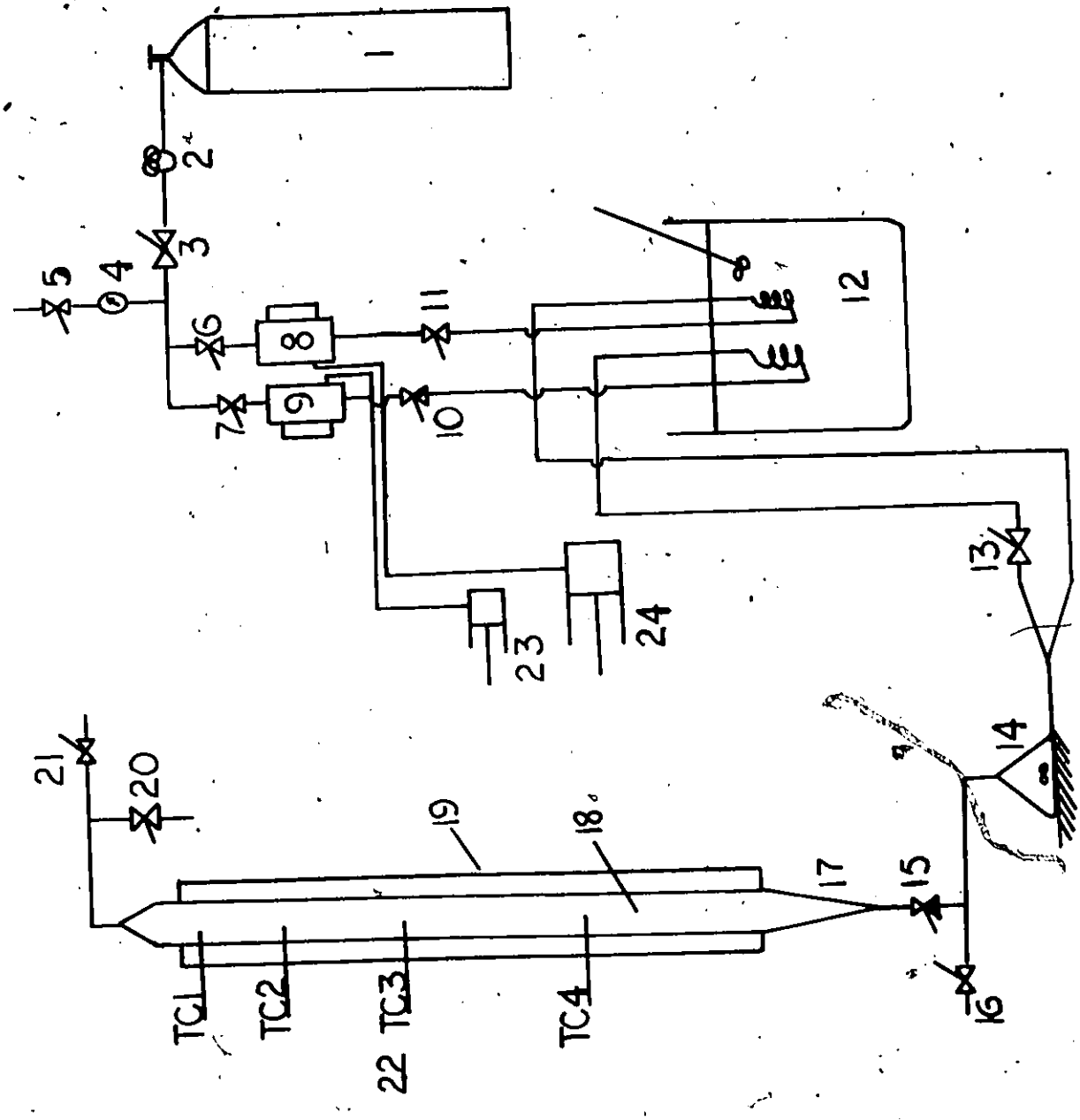

FIGURE 1-SCHEMATIC LAYOUT OF EQUIPMENT

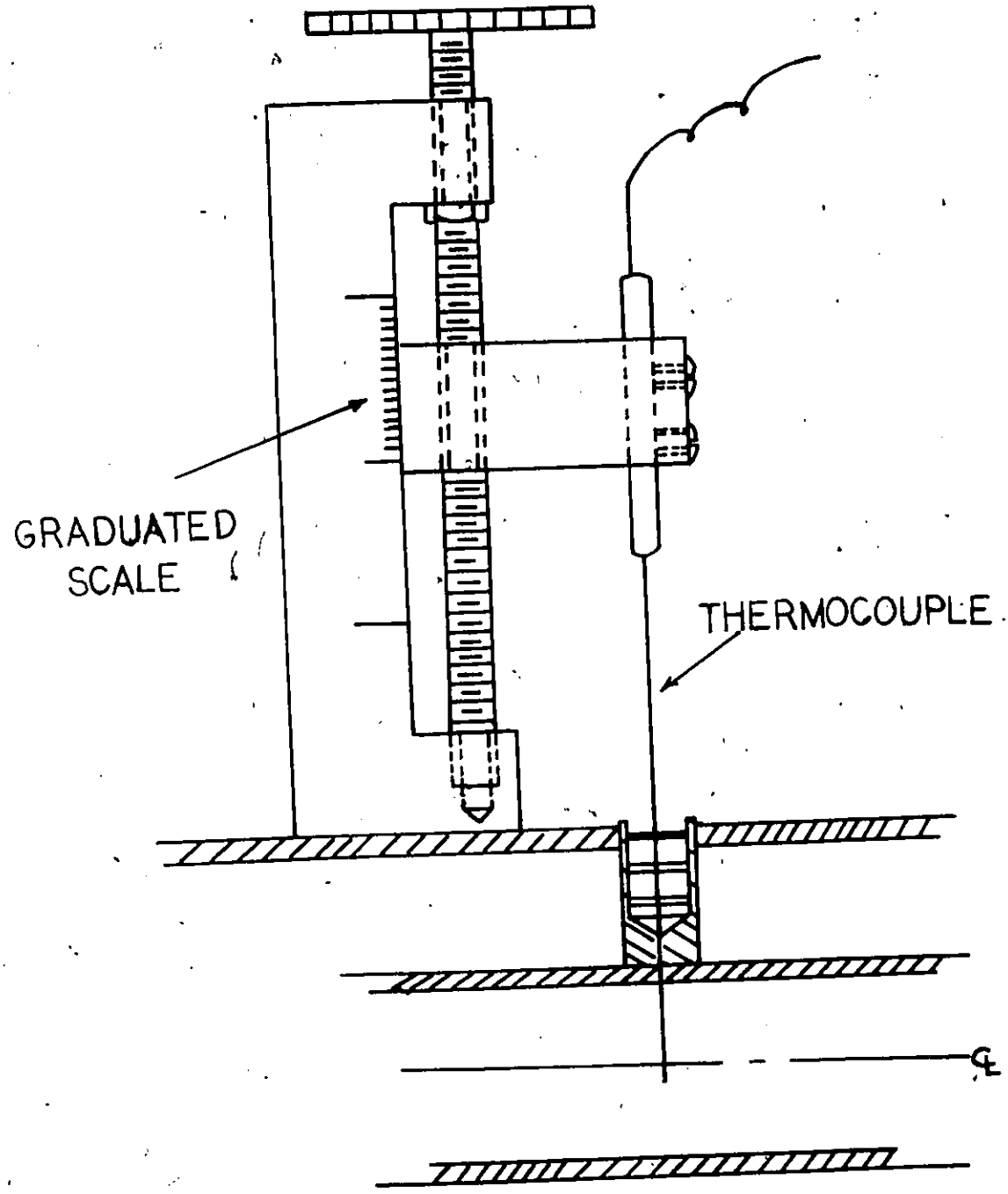

FIGURE 2 - TRAVERSING MECHANISM

separation. The reactor was jacketed and assumed to be operating under adiabatic conditions. A magnetic mixing chamber of 25 ml. capacity was placed at the inlet to the conical section of the reactor.

Temperature measurements were made with a copper-constantan probes of 13.2 cm. in length. The probes were mounted on a traversing mechanism (figure II) such that a radial traverse could be made. The thermocouples were located 35 cm, 100cm, 163 cm, and 191 cm from the end of the conical section. Readings were taken at the wall and at distances of 1/16", 1/8", 3/16", 3/8", 4/8", 5/8", 11/16 (CL) from the wall and at the same intervals from the centerline position to the opposite wall.

C. - Experimental Procedure

The reactants were first pumped (23 and 24) to their respective surge tanks (9 and 8). Pressure in the surge tanks was maintained at around 4-5 psig. by use of compressed air (1). Absorption of air into the reactants was reduced by use of a layer of oil which separated the reactants from the gas phase. This was found to be necessary to prevent formation of gas bubbles in the reactor. In addition the acetic anhydride was degassed before being pumped to the surge tank. This was accomplished by pre-heating the anhydride to 30°C and stripping with helium.

After the surge tanks, the reactants were preheated to 29°C (12) and then mixed in a magnetic stirring chamber (14) before entering the bottom of the reactor. The reaction was then allowed to come to steady state as indicated by temperature measurements near the outlet to the reactor. Acetic anhydride concentrations were determined by the aniline-water method (see Appendix C), and were taken at points (16) and (20).

V - RESULTS AND DISCUSSION

Theoretical and experimental results are shown in figures (3) to (26) for the following basic parameters

G_1 = 0.0078

G_2 = 17.704

G_3 = 2.866×10^8

G_4 - varying from 0.0310 to 0.0200

Variation of variables was achieved by changes in inlet concentration (C_{A_o}) from 0.706 to 0.455 (g.moles/litre) and Reynolds Number from 135 to 218.

The theoretical radial concentration and temperature profiles are shown in figures 3 to 14. For plug flow the profiles were constant in the radial direction but for laminar flow, the profiles varied. At low axial distances, the concentration x (fraction of reactant unconverted) was lower at the wall than at the centre due to the greater residence time at the wall. As the reaction proceeded, the reactant became depleted and the profiles tended to flatten. Correspondingly, the temperature profiles originally exhibited a maximum at the wall which shifted towards the centre as the reaction proceeded.

Nearly identical results were obtained for both laminar flow models. Thus, for low values of G_1, radial molecular diffusion did not significantly alter the radial profiles or conversions. A slight difference occured at low axial distances in the radial concentration profiles near the wall.

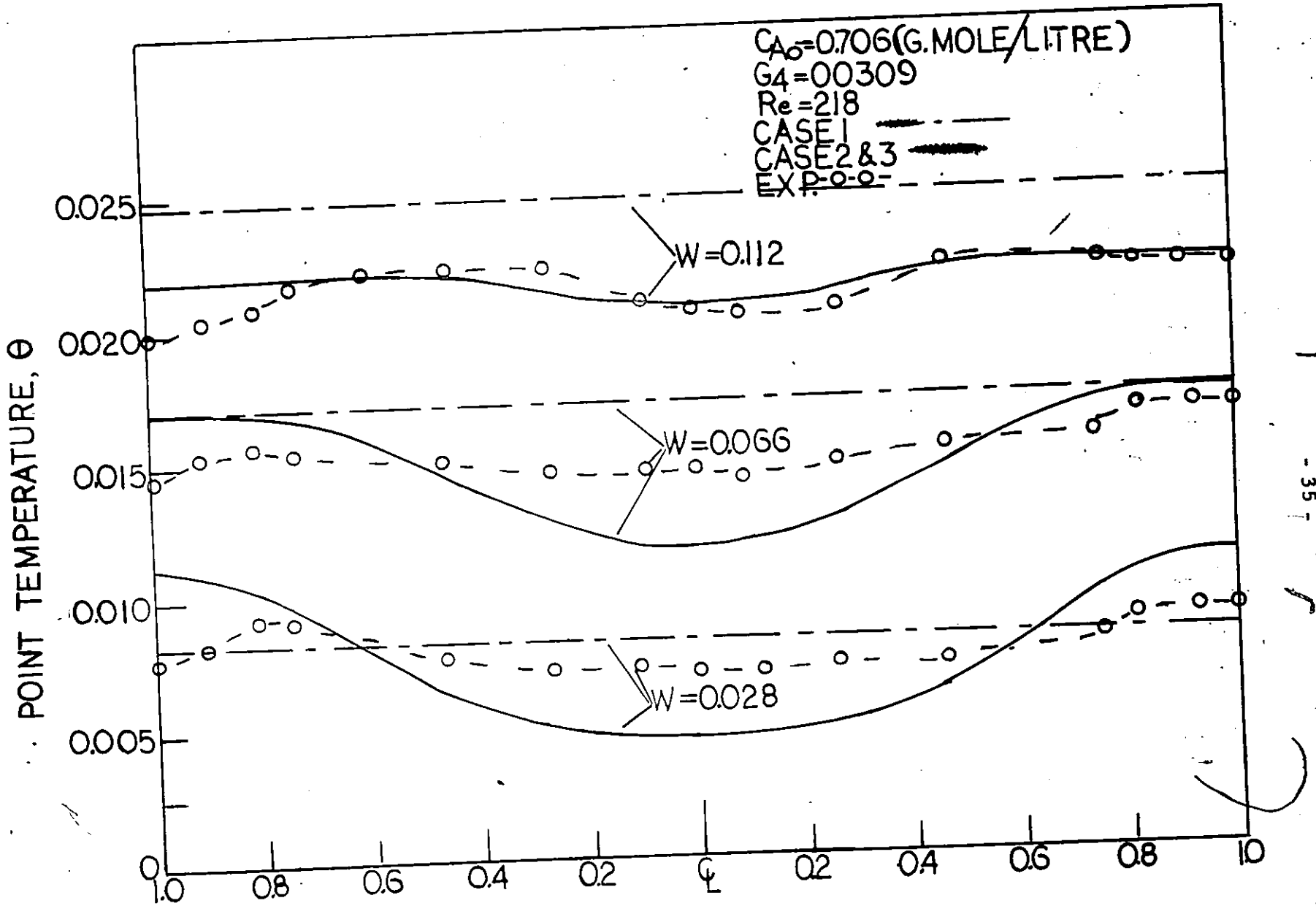
C_{A_0}=0.706(G.MOLE/LITRE)
G4=00309
Re=218
CASE1
CASE2&3
EXP.
W=0.112
W=0.066
W=0.028
POINT TEMPERATURE, θ
0.025
0.020
0.015
0.010
0.005
0
1.0
0.8
0.6
0.4
0.2
℄
0.2
0.4
0.6
0.8
1.0
RADIAL DISTANCE, a

FIGURE-3

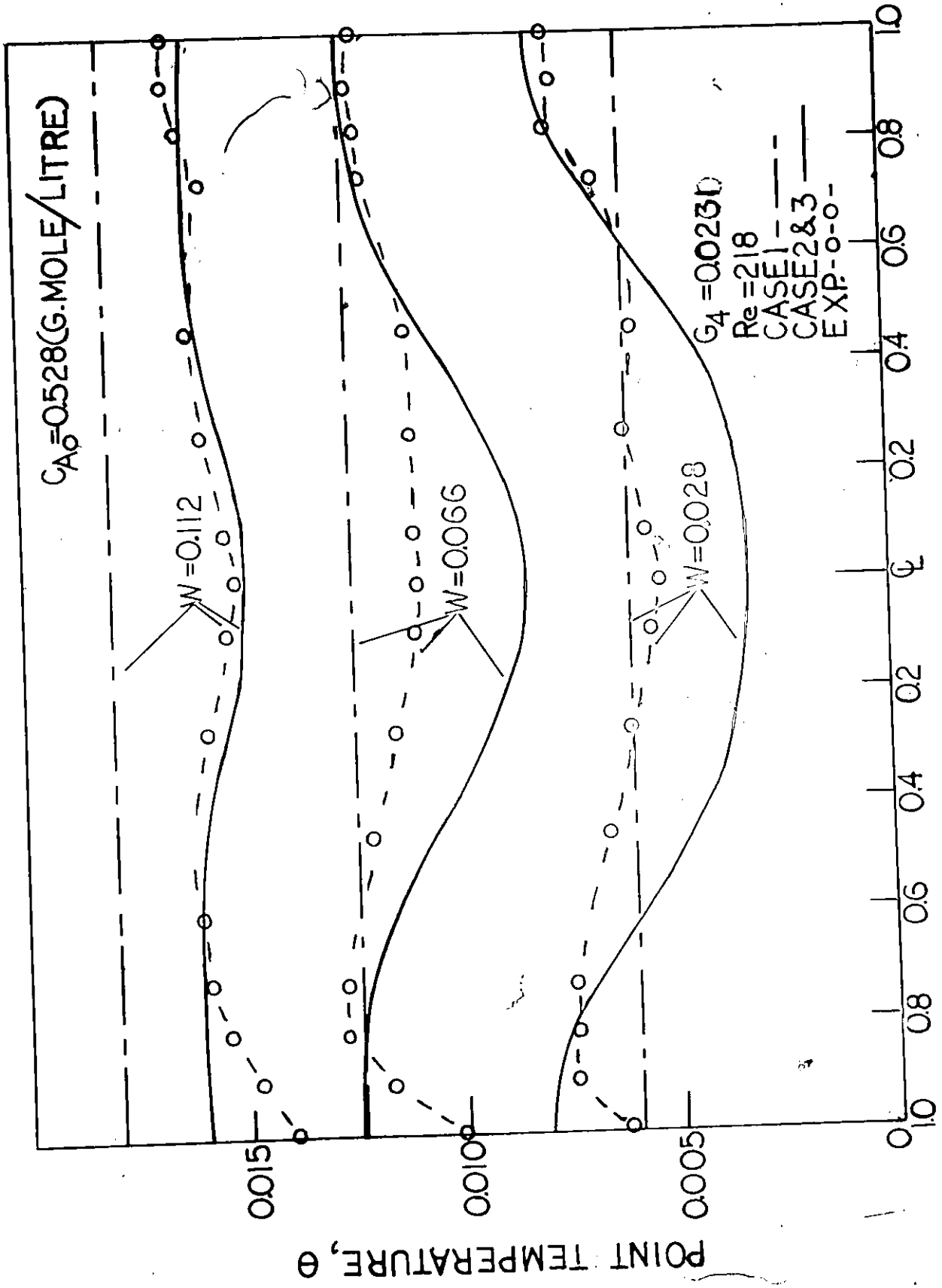
C_{A_0}=0.528(G.MOLE/LITRE)
W=0.112
W=0.066
W=0.028
G_4 =0.023
Re=218
CASE1 ——
CASE2&3 ——
EXP.-o-o-
POINT TEMPERATURE, θ
0.015
0.010
0.005
0
0.2
0.4
0.6
0.8
1.0
RADIAL DISTANCE, α

FIGURE-4

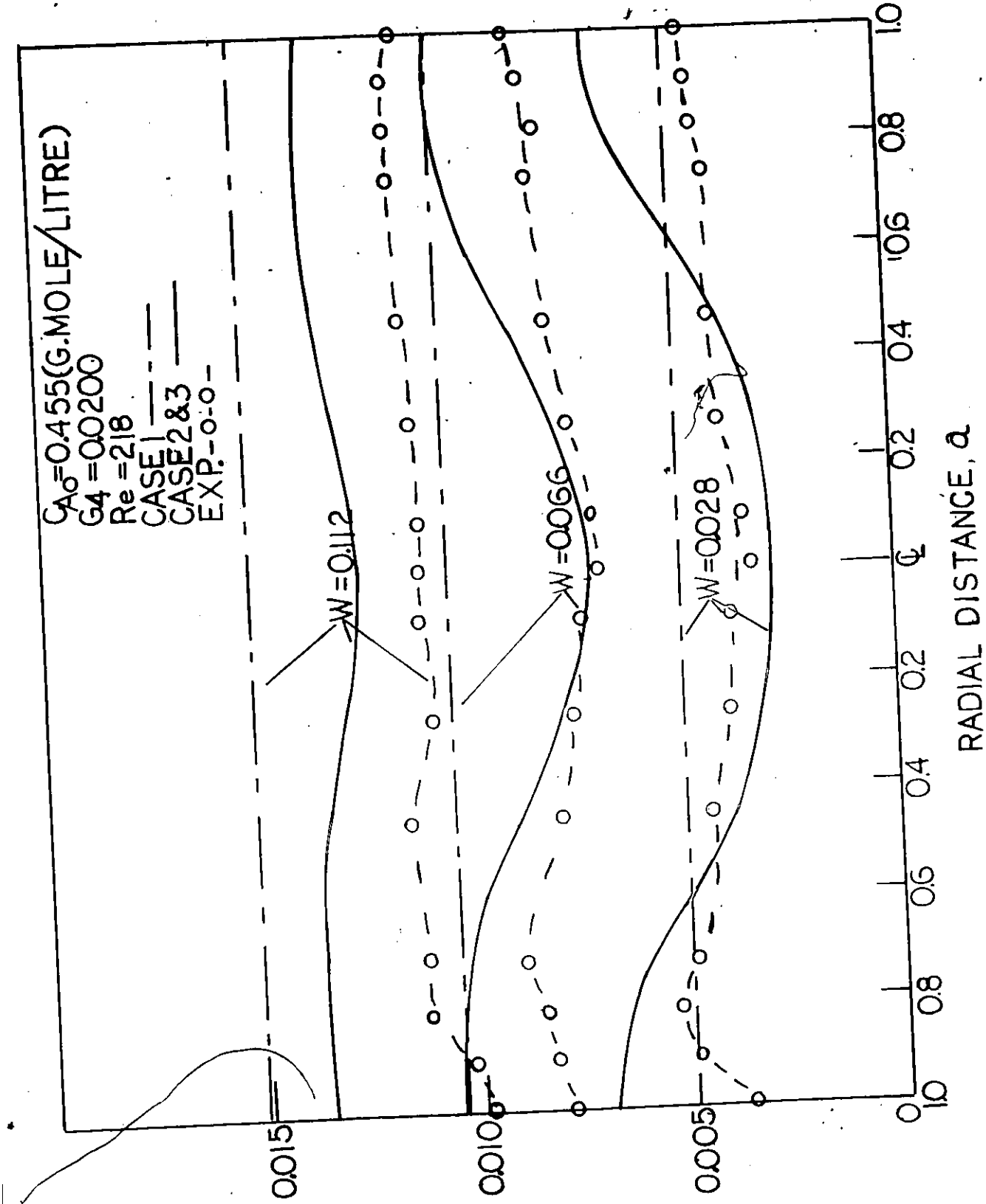
C_{A_0}=0.455(G.MOLE/LITRE)
G4 =0.0200
Re =218
CASE I
CASE 2&3
EXP.-o-o-
W=0.112
W=0.066
W=0.028
POINT TEMPERATURE, θ
RADIAL DISTANCE, α
0.015
0.010
0.005
0.0
0.2
0.4
0.6
0.8
1.0

FIGURE-5

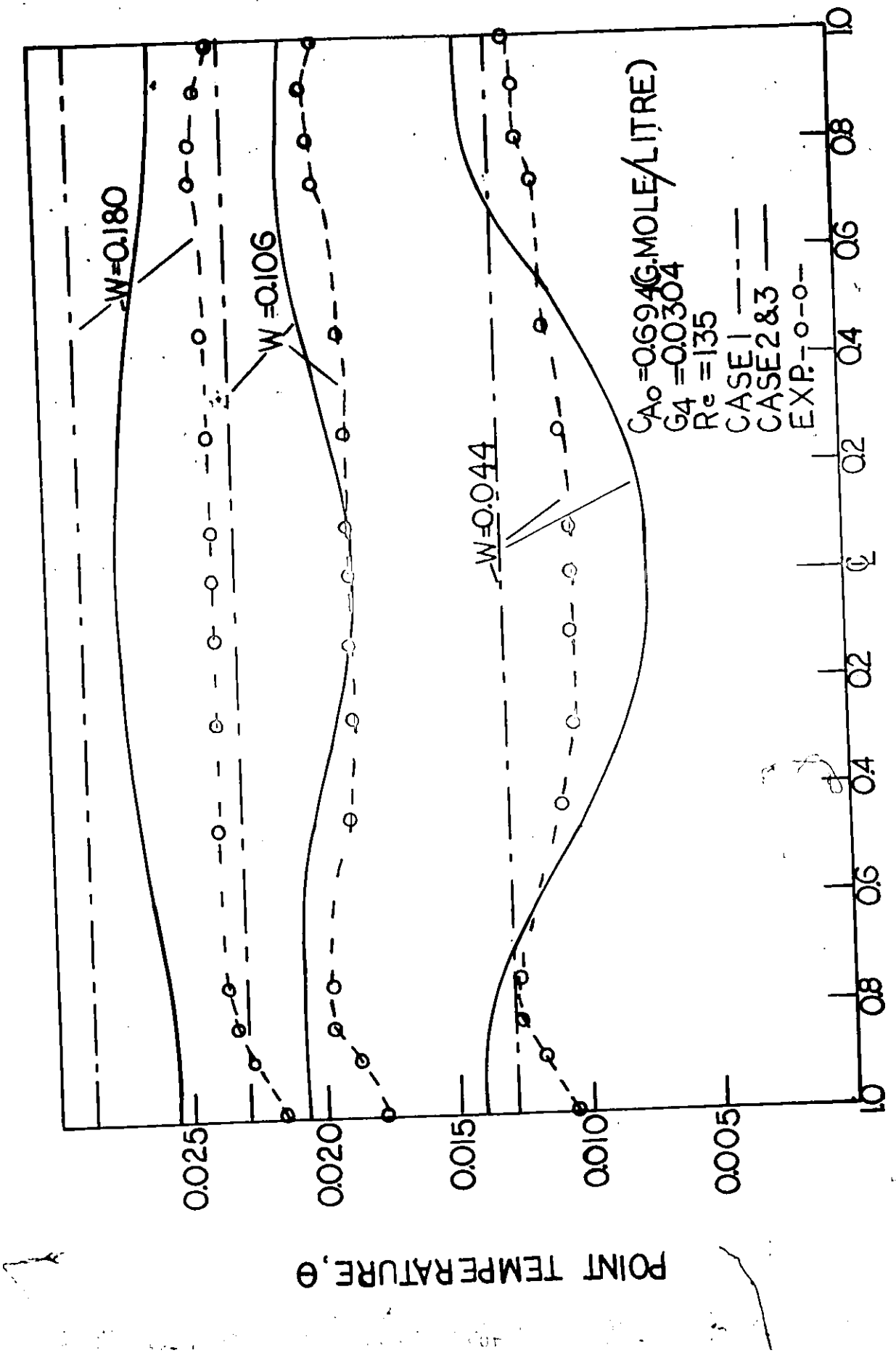
POINT TEMPERATURE, θ
0.025
0.020
0.015
0.010
0.005
W=0.180
W=0.106
W=0.044
C_{A_0} =0.6946 G.MOLE/LITRE)
G4 =0.0304
Re =135
CASE I
CASE 2&3
EXP.
1.0
0.8
0.6
0.4
0.2
0
0.2
0.4
0.6
0.8
1.0
RADIAL DISTANCE, a

FIGURE-6

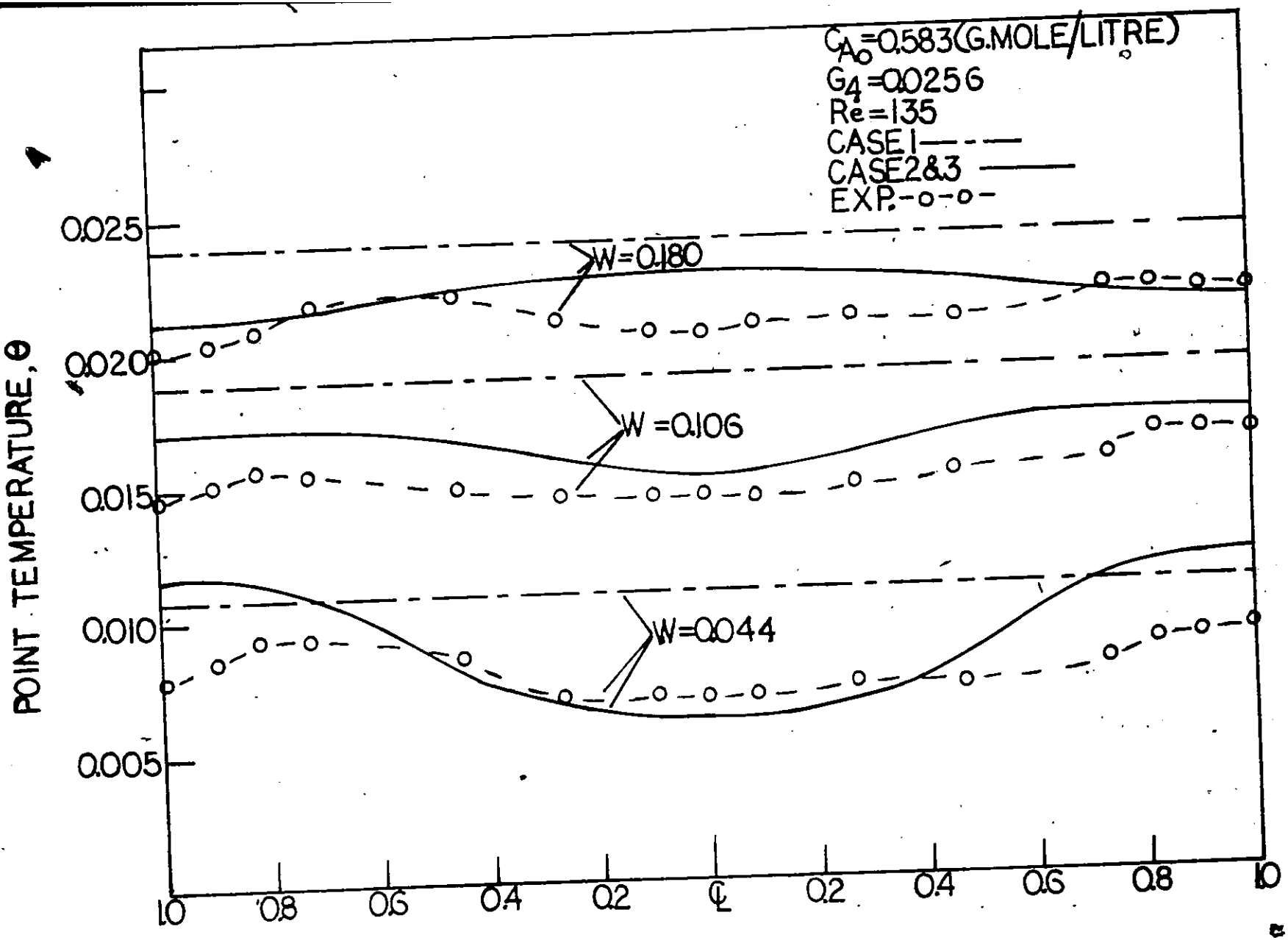
C_{A_0}=0.583(G.MOLE/LITRE)
G_4=0.0256
Re=135
CASE1
CASE2&3
EXP.
W=0.180
W=0.106
W=0.044
POINT TEMPERATURE, θ
0.025
0.020
0.015
0.010
0.005
1.0
0.8
0.6
0.4
0.2
℄
0.2
0.4
0.6
0.8
1.0
RADIAL DISTANCE, a

FIGURE-7

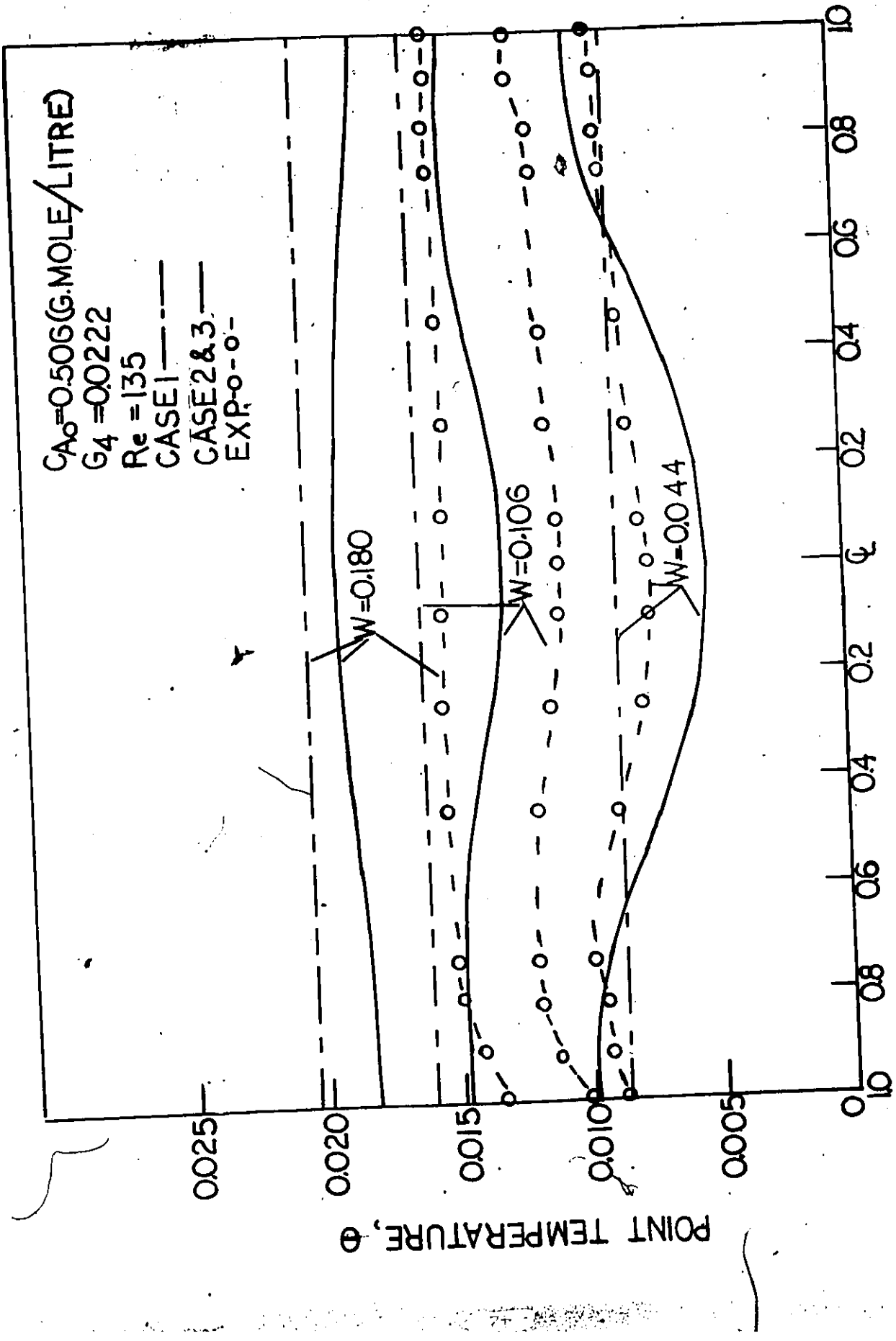
C_{A_0}=0.506(G.MOLE/LITRE)
G_4 =0.0222
Re =135
CASE1 ——
CASE2&3 ——
EXP-o-o-
W=0.180
W=0.106
W=0.044
POINT TEMPERATURE, θ
0.025
0.020
0.015
0.010
0.005
0
.1
.2
.4
.6
.8
1.0
RADIAL DISTANCE, α

FIGURE-8

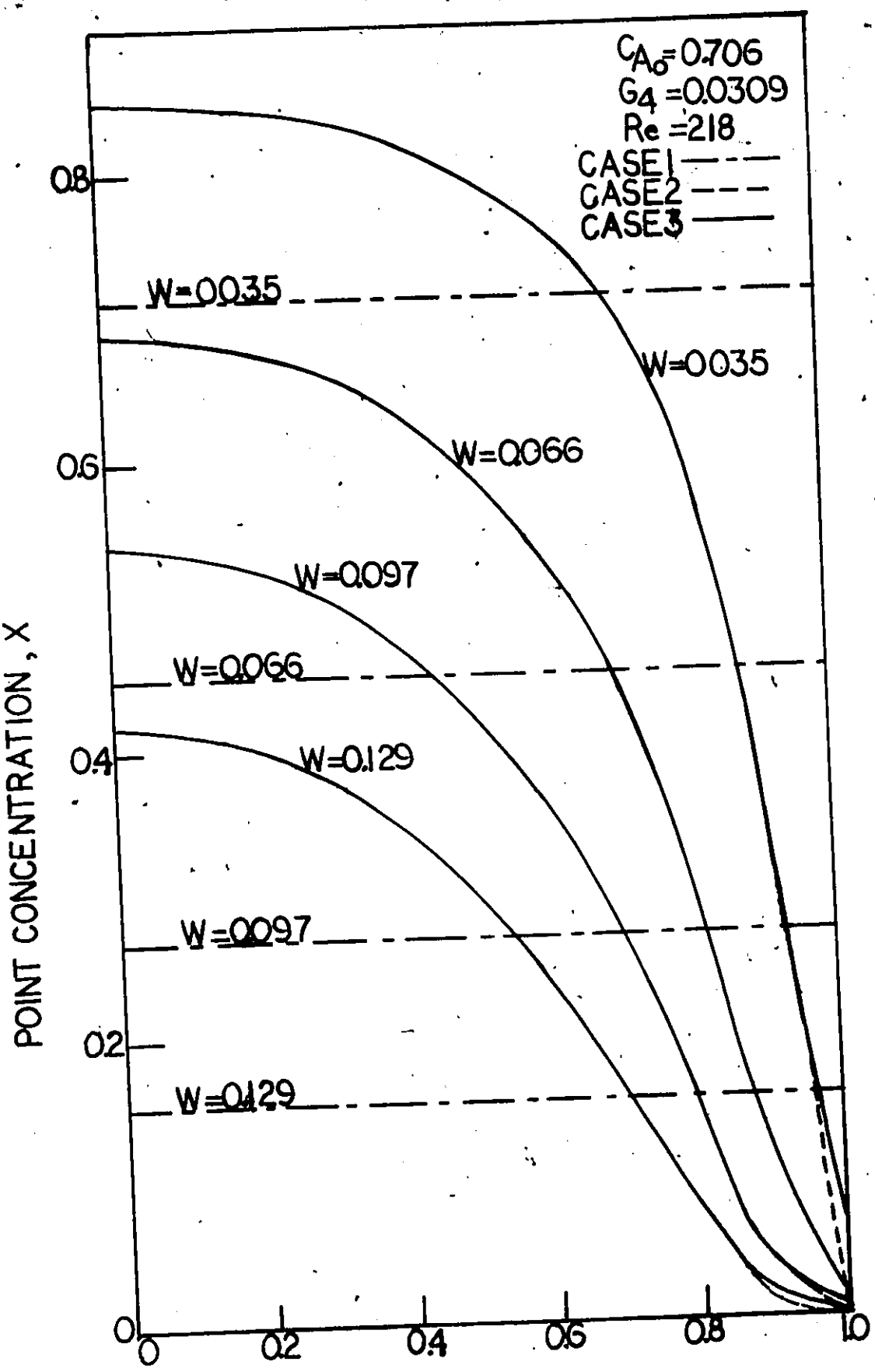
C_{A_0}=0.706
G_4=0.0309
Re =218
CASE1
CASE2
CASE3
W=0.035
W=0.066
W=0.097
W=0.129
W=0.035
W=0.066
W=0.097
W=0.129
0.8
0.6
0.4
0.2
0
0
0.2
0.4
0.6
0.8
1.0
POINT CONCENTRATION, X
RADIAL DISTANCE, a

FIGURE-9

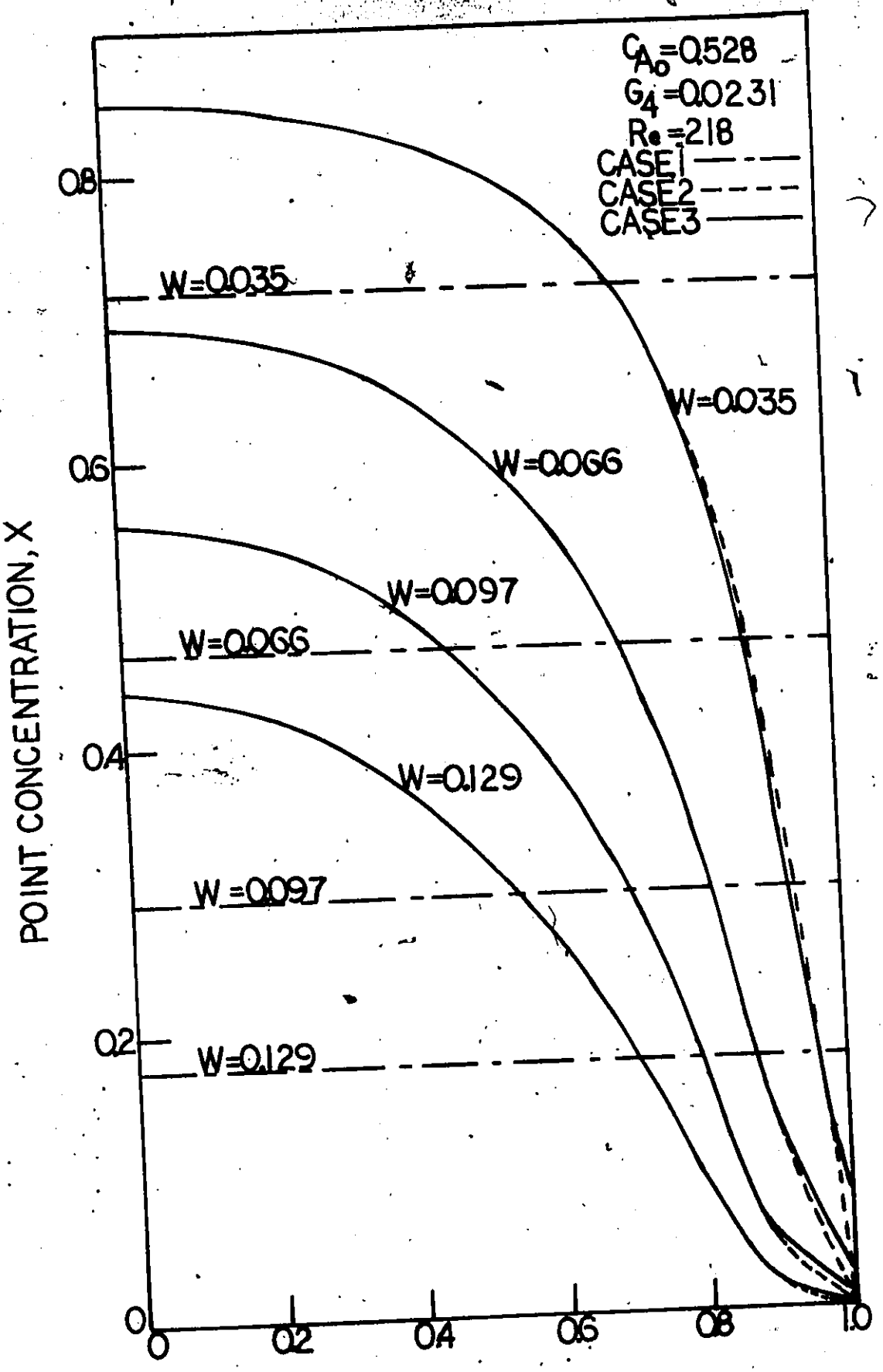
C_{A_o}=0.528
G_4=0.0231
R_e=218
CASE1
CASE2
CASE3
W=0.035
W=0.066
W=0.097
W=0.129
W=0.035
W=0.066
W=0.097
W=0.129
POINT CONCENTRATION, X
RADIAL DISTANCE, a
0
0.2
0.4
0.6
0.8
1.0

FIGURE-10

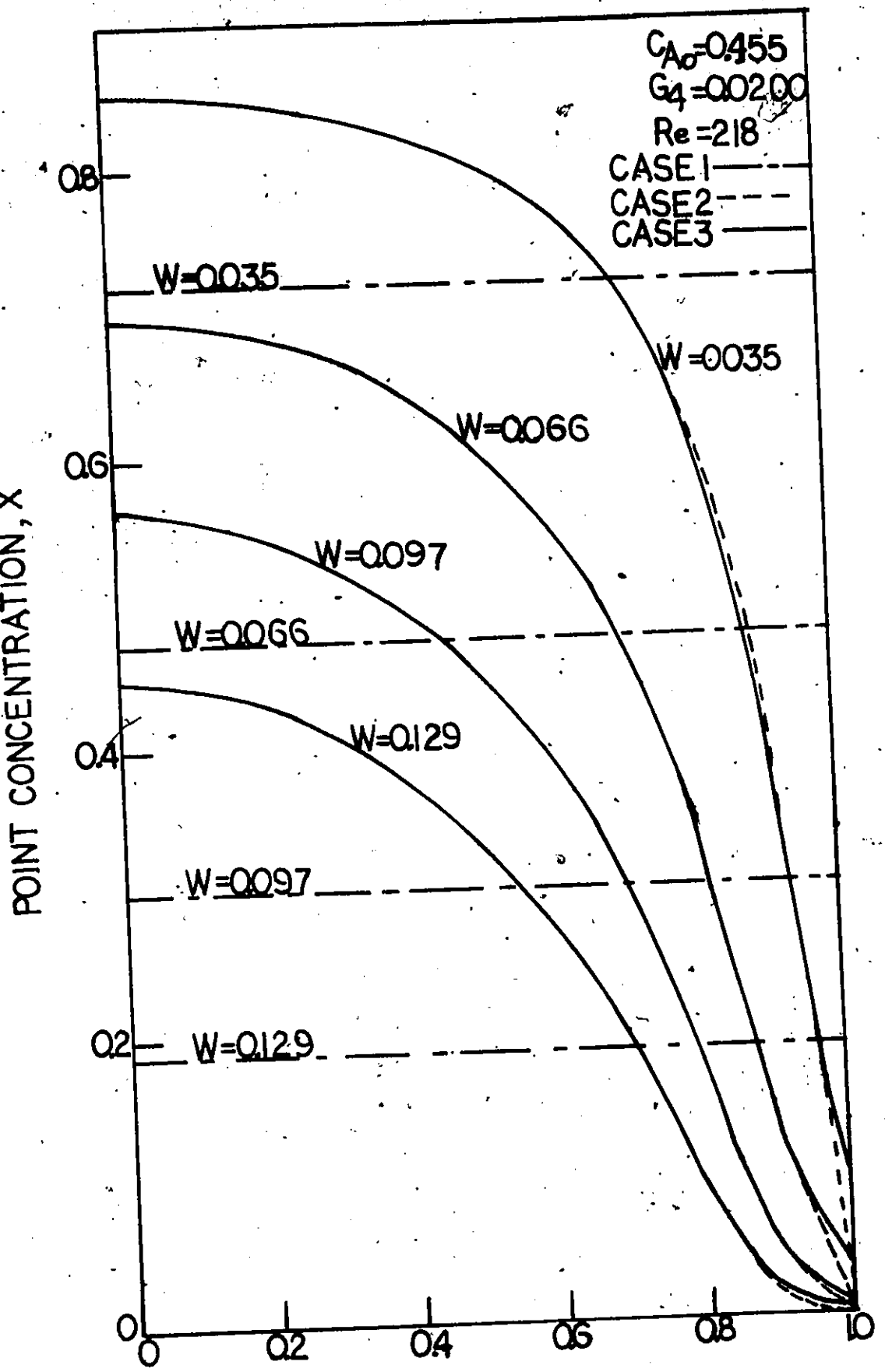
C_{A_0}=0.455
G_4=0.0200
Re=218
CASE 1
CASE 2
CASE 3
W=0.035
W=0.066
W=0.097
W=0.129
W=0.035
W=0.066
W=0.097
W=0.129
0.8
0.6
0.4
0.2
0
0
0.2
0.4
0.6
0.8
1.0
POINT CONCENTRATION, X
RADIAL DISTANCE, a

FIGURE-11

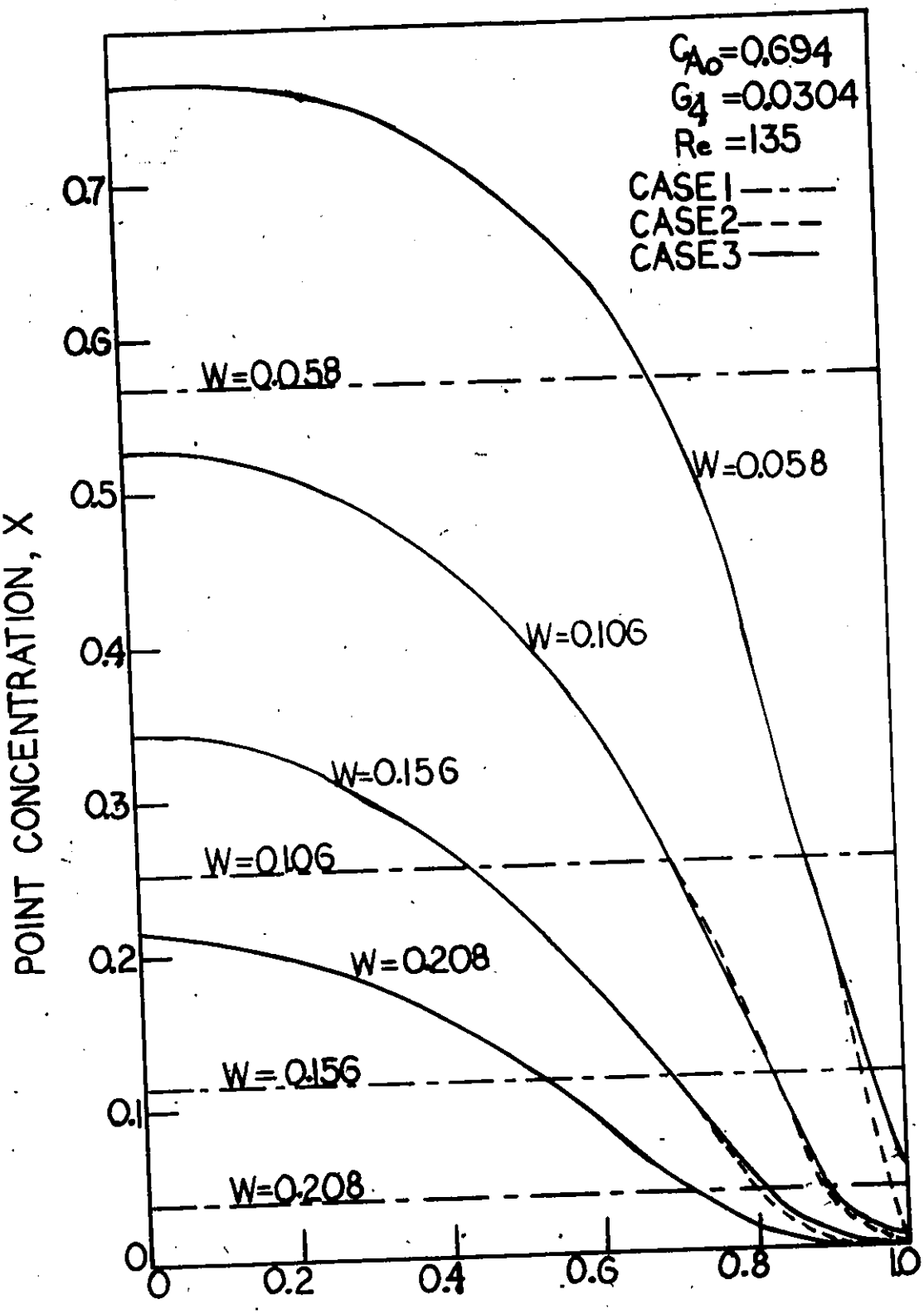
C_{A_0}=0.694
G_4 =0.0304
Re =135
CASE 1
CASE 2
CASE 3
W=0.058
W=0.106
W=0.156
W=0.208
W=0.058
W=0.106
W=0.156
W=0.208
POINT CONCENTRATION, X
RADIAL DISTANCE, a
0
0.1
0.2
0.3
0.4
0.5
0.6
0.7
0.2
0.4
0.6
0.8
1.0

FIGURE-12

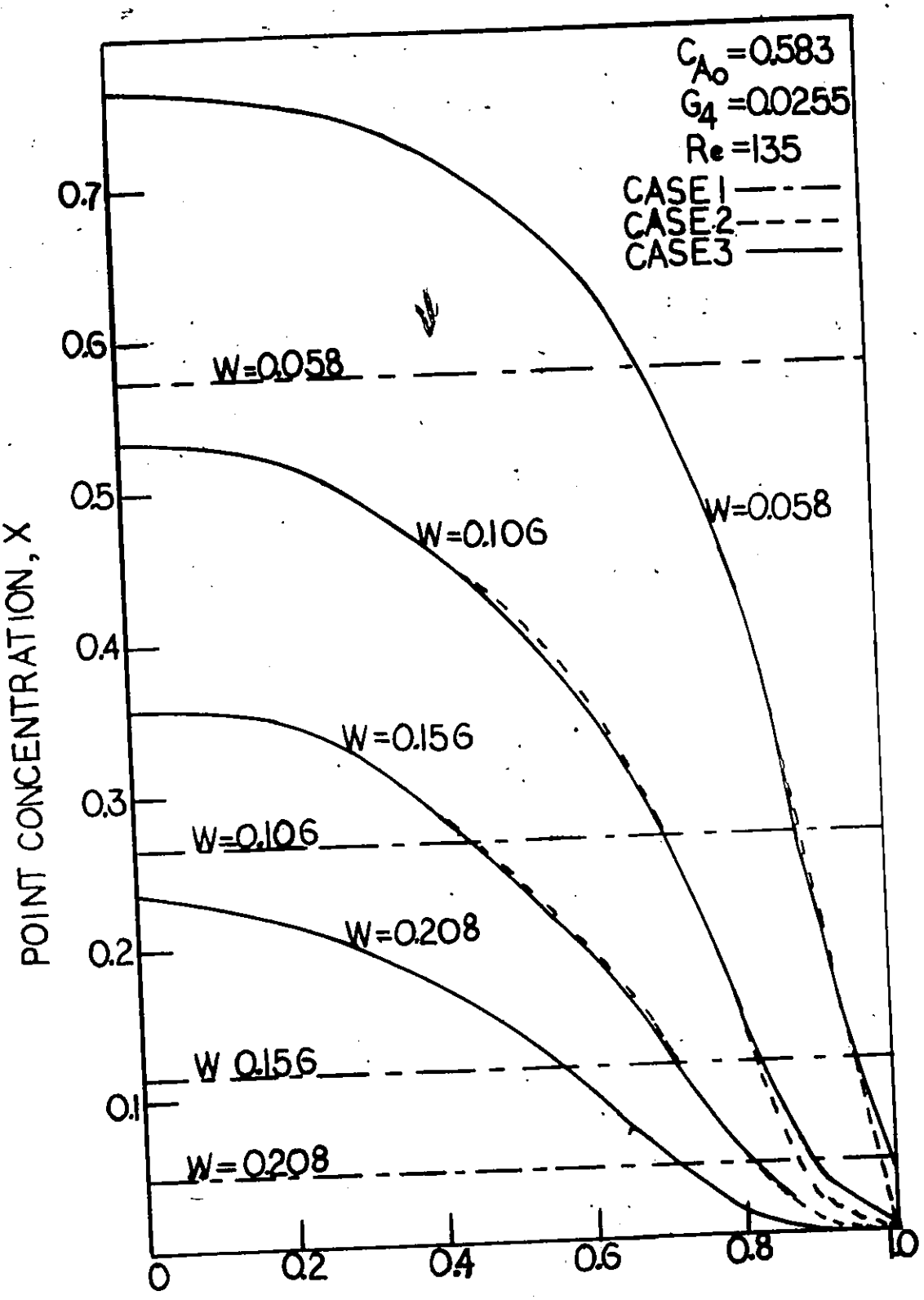
C_{A_o}=0.583
G_4=0.0255
Re=135
CASE 1
CASE 2
CASE 3
W=0.058
W=0.106
W=0.156
W=0.208
W=0.058
W=0.106
W 0.156
W=0.208
POINT CONCENTRATION, X
RADIAL DISTANCE, a
0.7
0.6
0.5
0.4
0.3
0.2
0.1
0
0.2
0.4
0.6
0.8
1.0

FIGURE-13

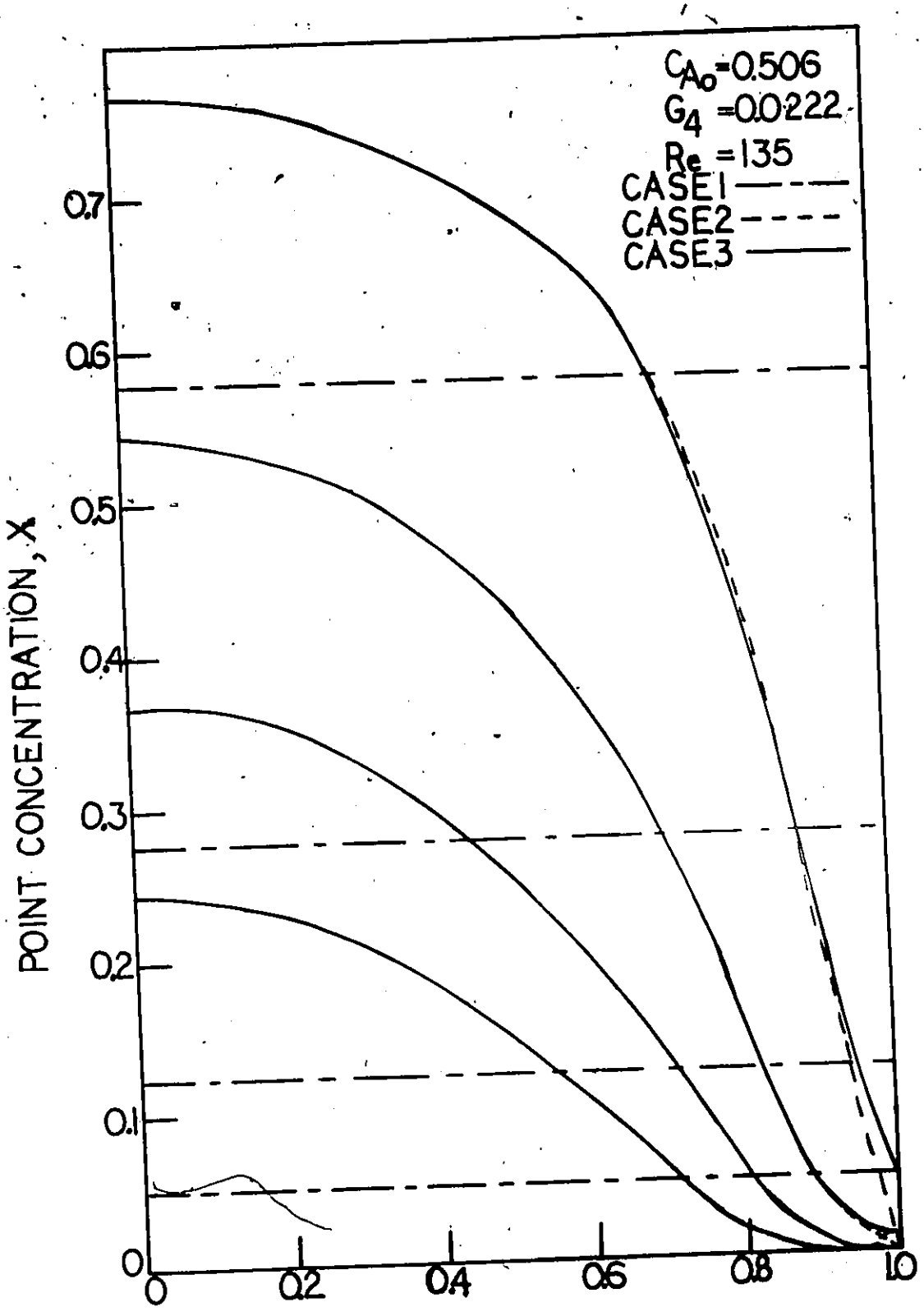
C_{A_0}=0.506
G_4 =0.0222
R_e =135
CASE1
CASE2
CASE3
POINT CONCENTRATION, X
0.7
0.6
0.5
0.4
0.3
0.2
0.1
0
0
0.2
0.4
0.6
0.8
1.0
RADIAL DISTANCE, a

FIGURE-14

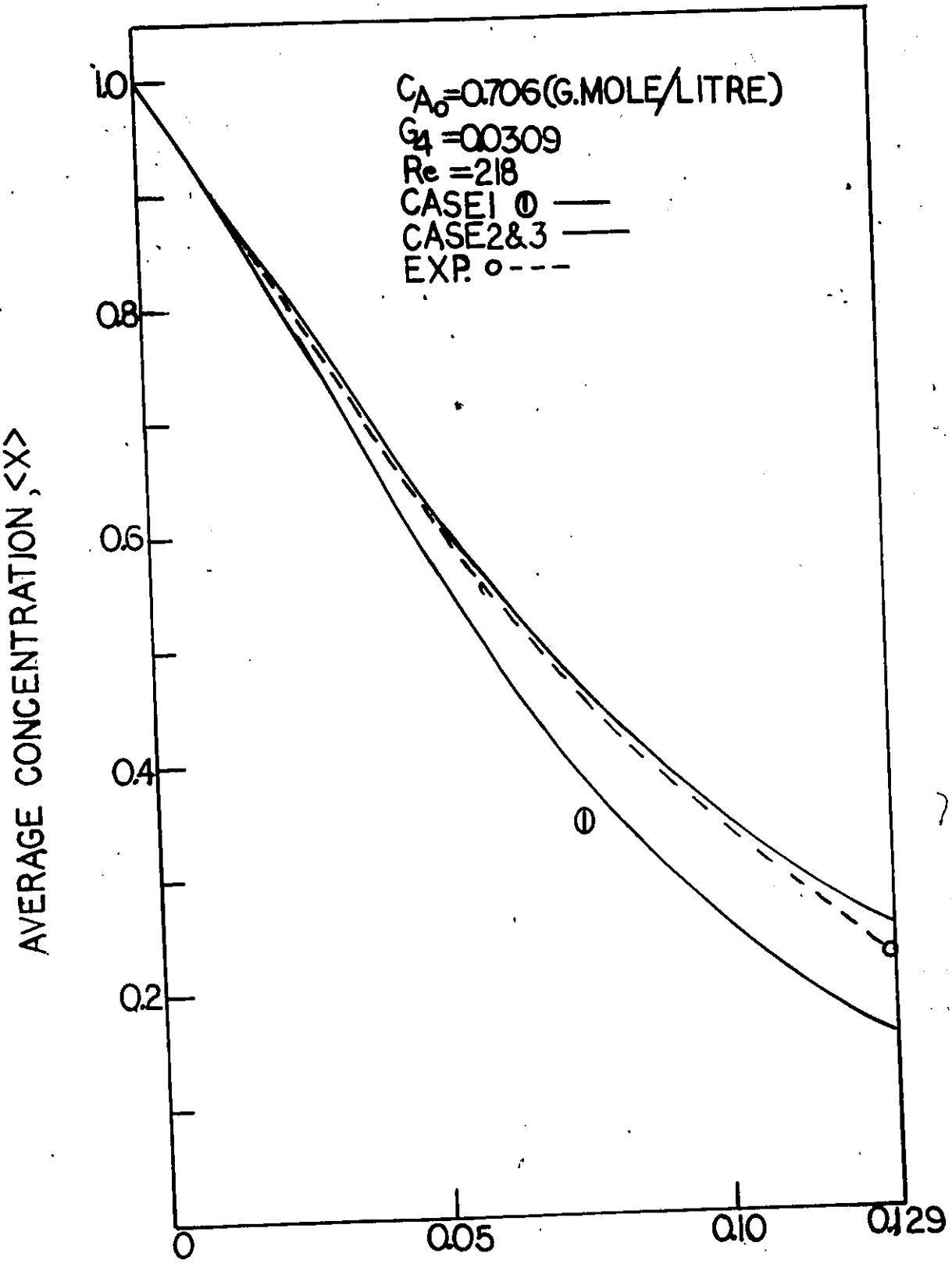
C_{A_0}=0.706(G.MOLE/LITRE)
G_4 =0.0309
Re =218
CASE1 ① ——
CASE2&3 ——
EXP. o---
1.0
0.8
0.6
0.4
0.2
0
0.05
0.10
0.129
①
②
AVERAGE CONCENTRATION, <X>
AXIAL DISTANCE, W

FIGURE-15

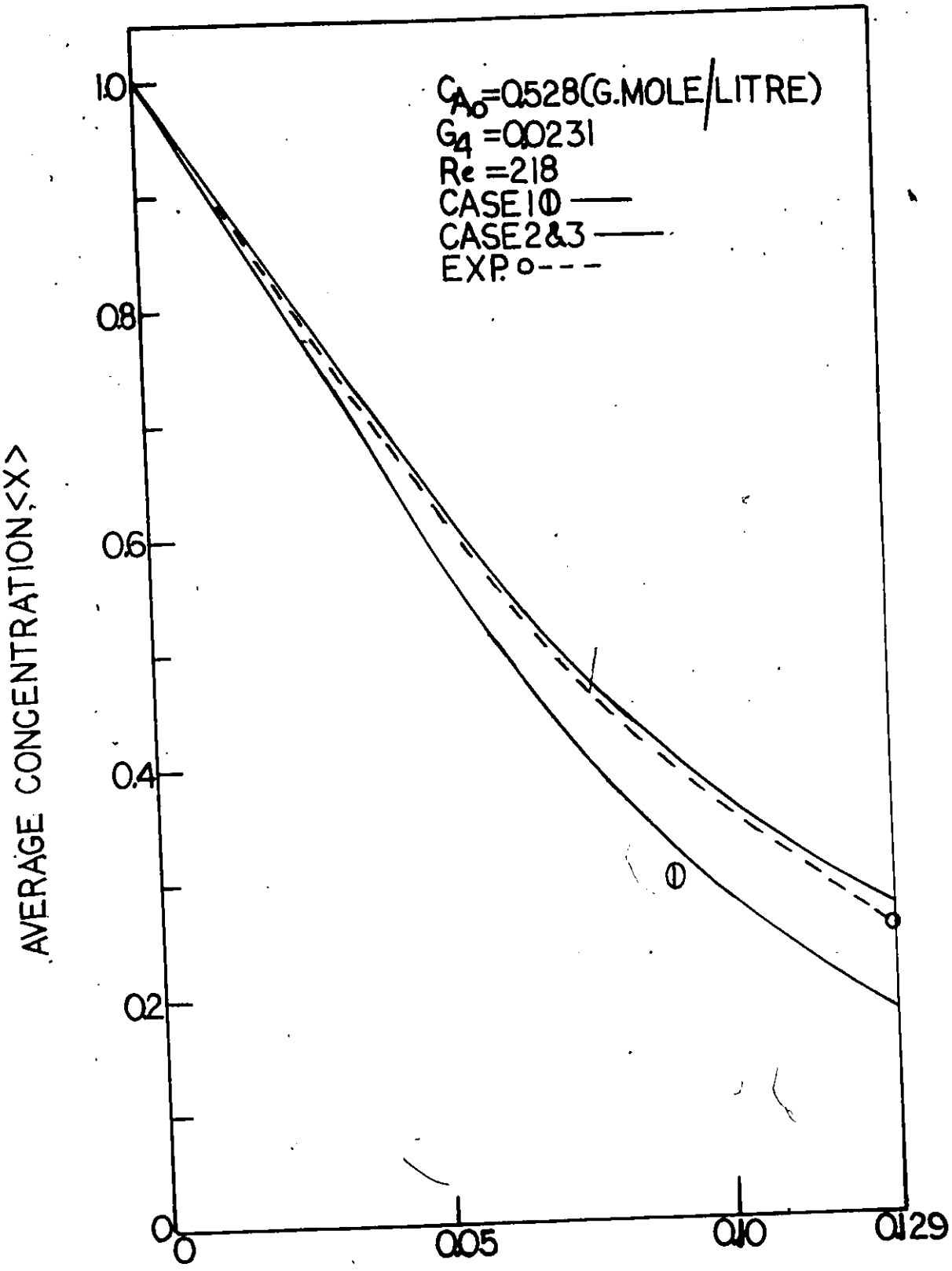
C_{A_0}=0.528(G.MOLE/LITRE)
G_4 =0.0231
Re =218
CASE1① ——
CASE2&3 ——
EXP. o - - -
1.0
0.8
0.6
0.4
0.2
0
0
0.05
0.10
0.129
①
AVERAGE CONCENTRATION, <X>
AXIAL DISTANCE, W

FIGURE-16

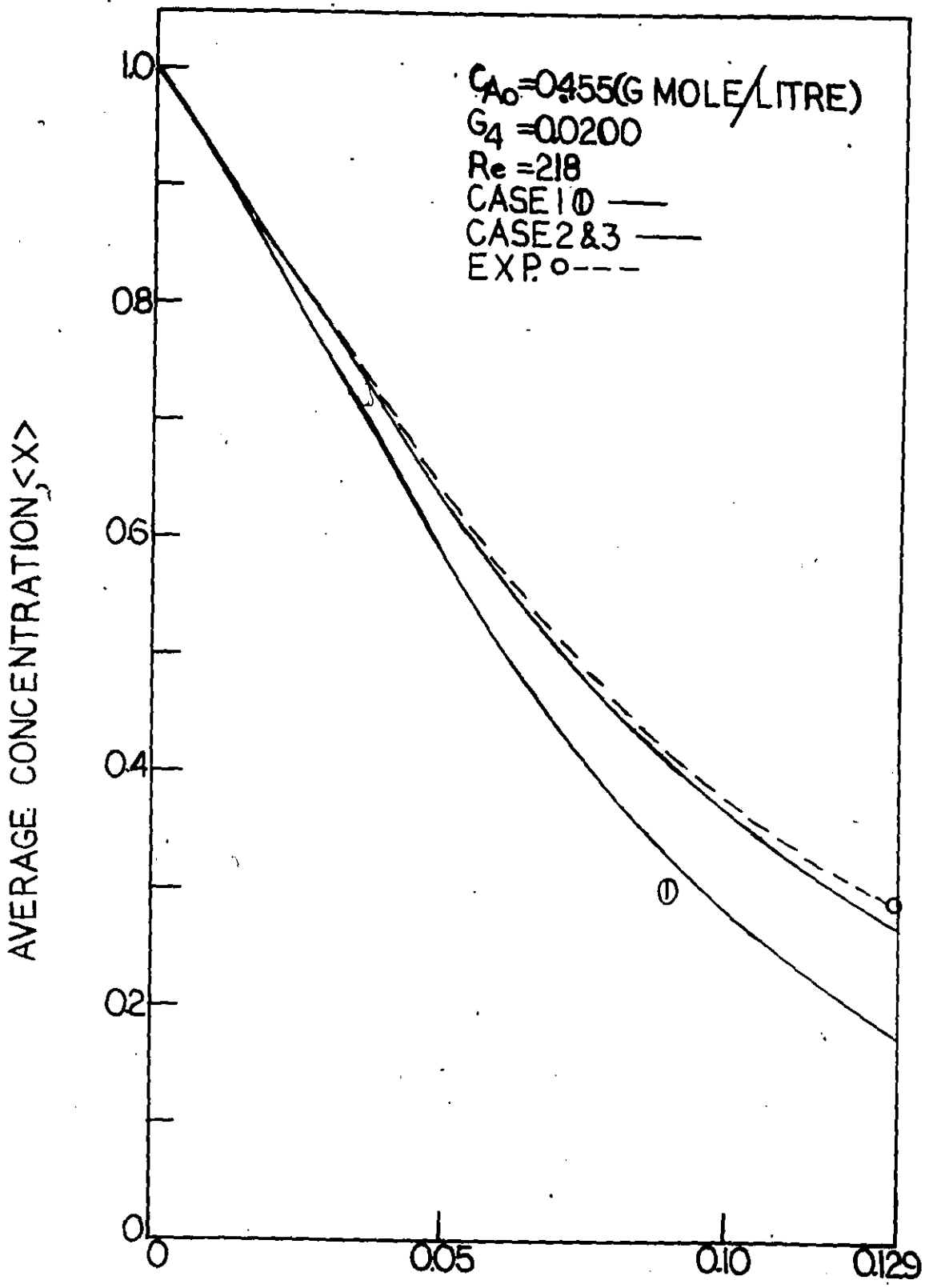
C_{A_0}=0.455(G MOLE/LITRE)
G_4 =0.0200
Re =218
CASE 1 ①
CASE 2 & 3
EXP. o
AVERAGE CONCENTRATION, <X>
1.0
0.8
0.6
0.4
0.2
0
0
0.05
0.10
0.129
①
AXIAL DISTANCE, W

FIGURE-17

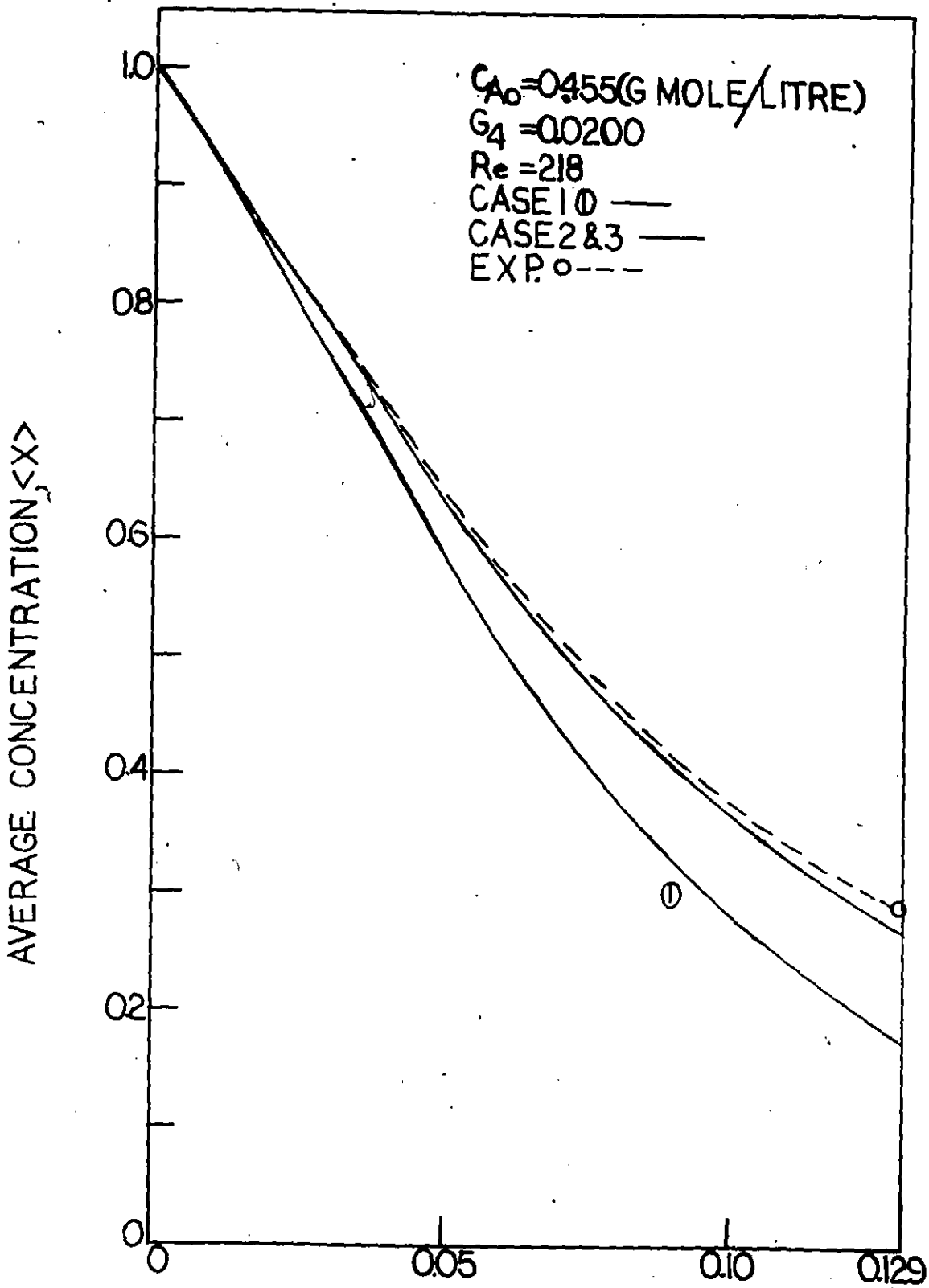
C_{A_0}=0.455(G MOLE/LITRE)
G_4 =0.0200
Re =218
CASE 1① ——
CASE 2&3 ——
EXP. o---
AVERAGE CONCENTRATION, <X>
1.0
0.8
0.6
0.4
0.2
0
0
0.05
0.10
0.129
①
AXIAL DISTANCE, W

FIGURE-17

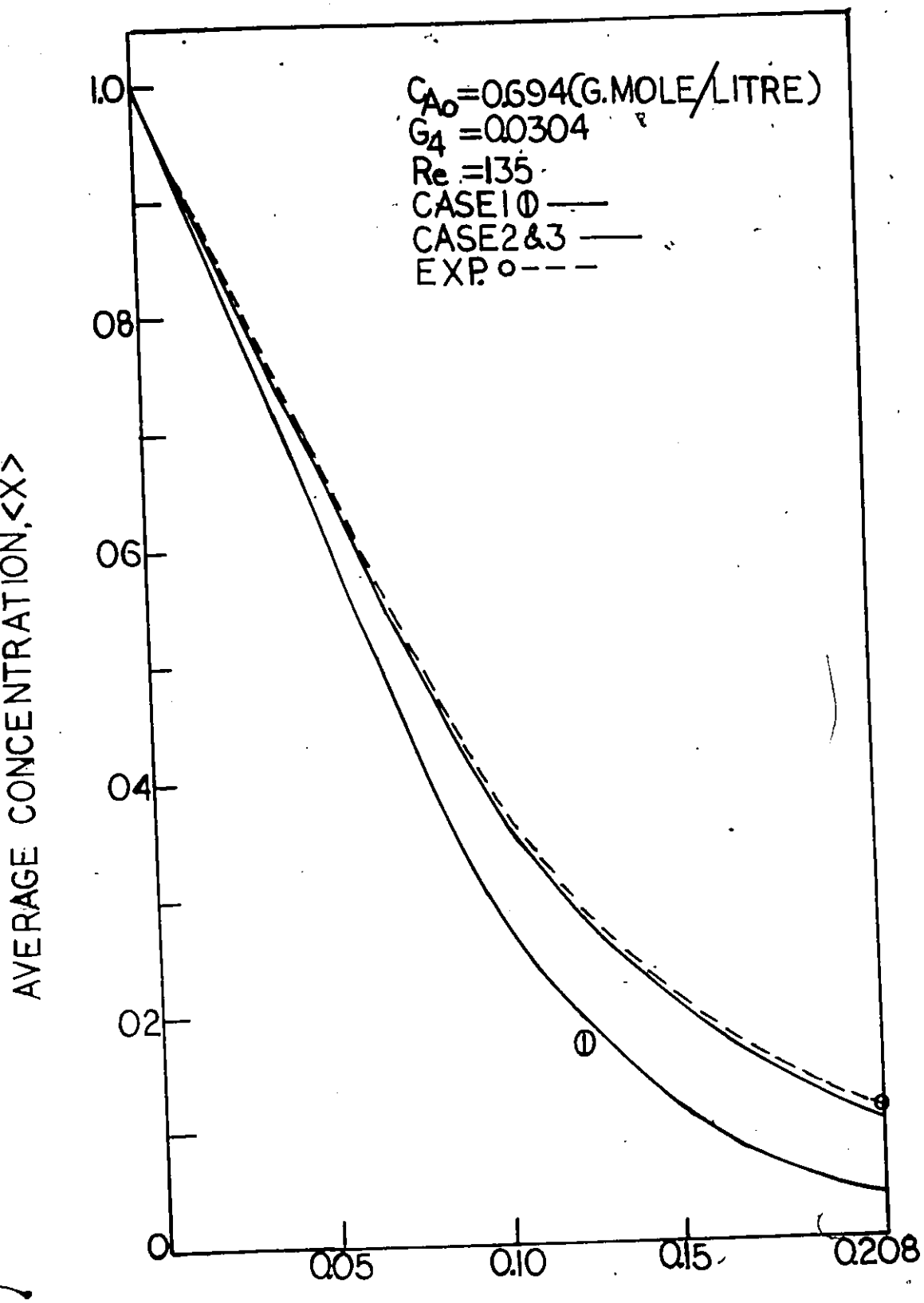
C_{A_o}=0.694(G.MOLE/LITRE)
G_4 =0.0304
Re =135
CASE1 ①——
CASE2&3 ——
EXP. o---
1.0
08
06
04
02
0
0.05
0.10
0.15
0.208
①
AVERAGE CONCENTRATION, <X>
AXIAL DISTANCE, W

FIGURE-18

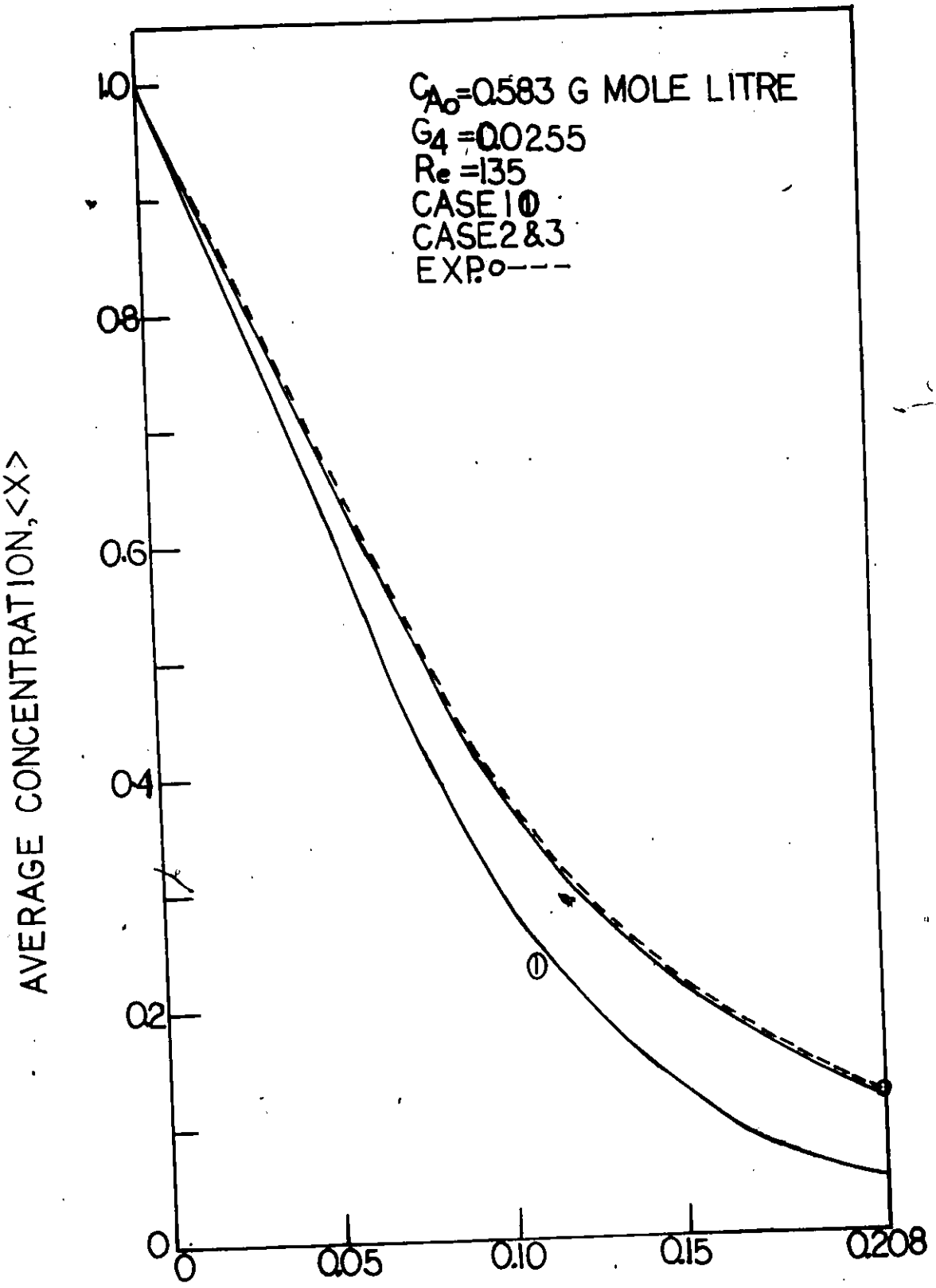
C_{A_0}=0.583 G MOLE LITRE
G_4 =0.0255
Re =135
CASE 1①
CASE 2&3
EXP.o---
AVERAGE CONCENTRATION, <X>
1.0
0.8
0.6
0.4
0.2
0
0
0.05
0.10
0.15
0.208
① AXIAL DISTANCE, W

FIGURE-19

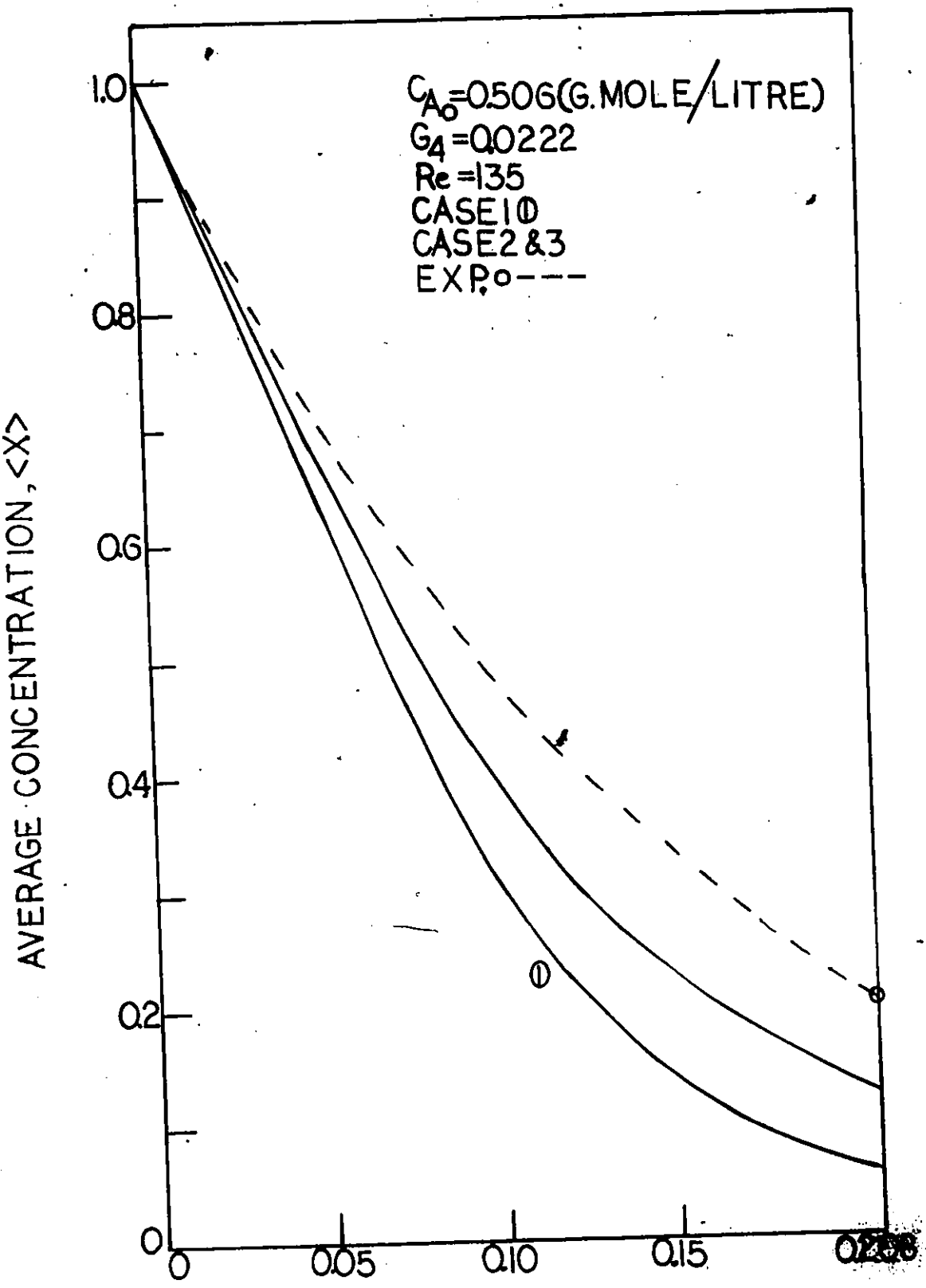
C_{A_0}=0.506(G.MOLE/LITRE)
G_4=0.0222
Re=135
CASE1①
CASE2&3
EXP.o---
AVERAGE CONCENTRATION, <X>
1.0
0.8
0.6
0.4
0.2
0
0
0.05
0.10
0.15
0.20
AXIAL DISTANCE, W

FIGURE-20

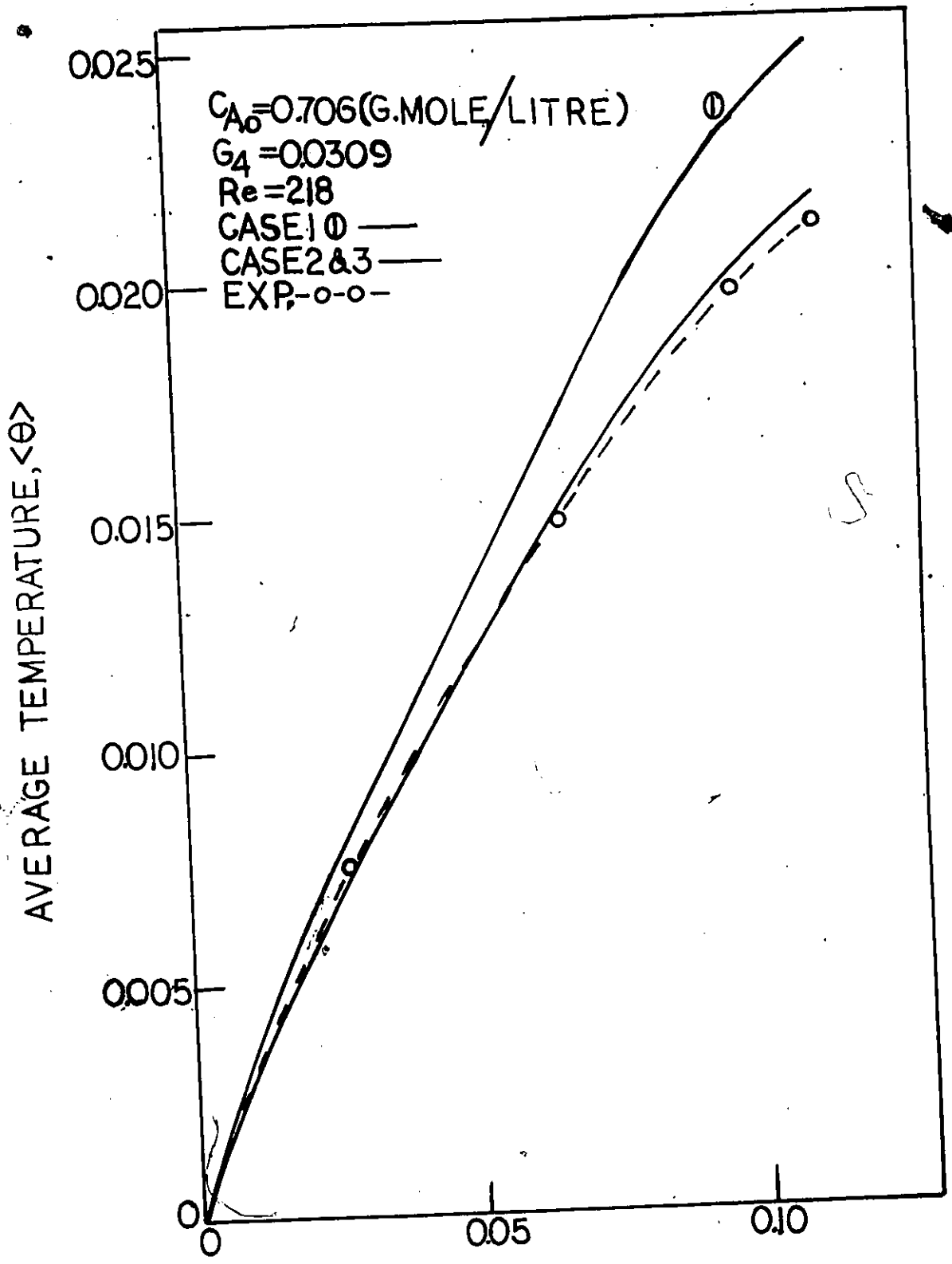
0.025
0.020
0.015
0.010
0.005
0
0
0.05
0.10
C_{A_0}=0.706(G.MOLE/LITRE)
G_4=0.0309
Re=218
CASE1 ① ——
CASE2&3 ——
EXP.-o-o-
①
AVERAGE TEMPERATURE, <θ>
AXIAL DISTANCE, W

FIGURE-21

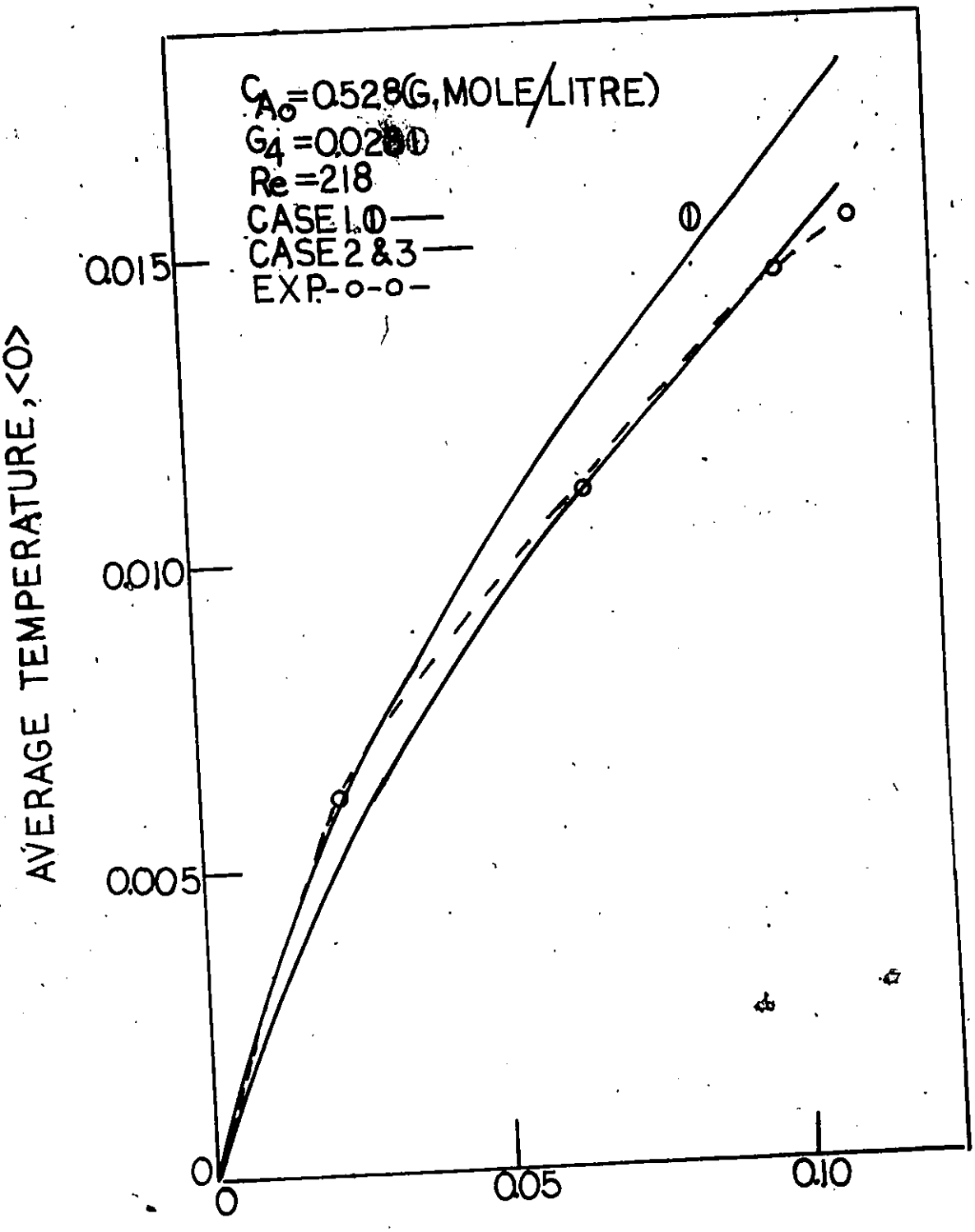
C_{A_0}=0.528(G, MOLE/LITRE)
G_4=0.0280
Re=218
CASE 1.0 —
CASE 2 & 3 —
EXP.-o-o-
AVERAGE TEMPERATURE, <O>
0.015
0.010
0.005
0
0
0.05
0.10
AXIAL DISTANCE, W

FIGURE-22

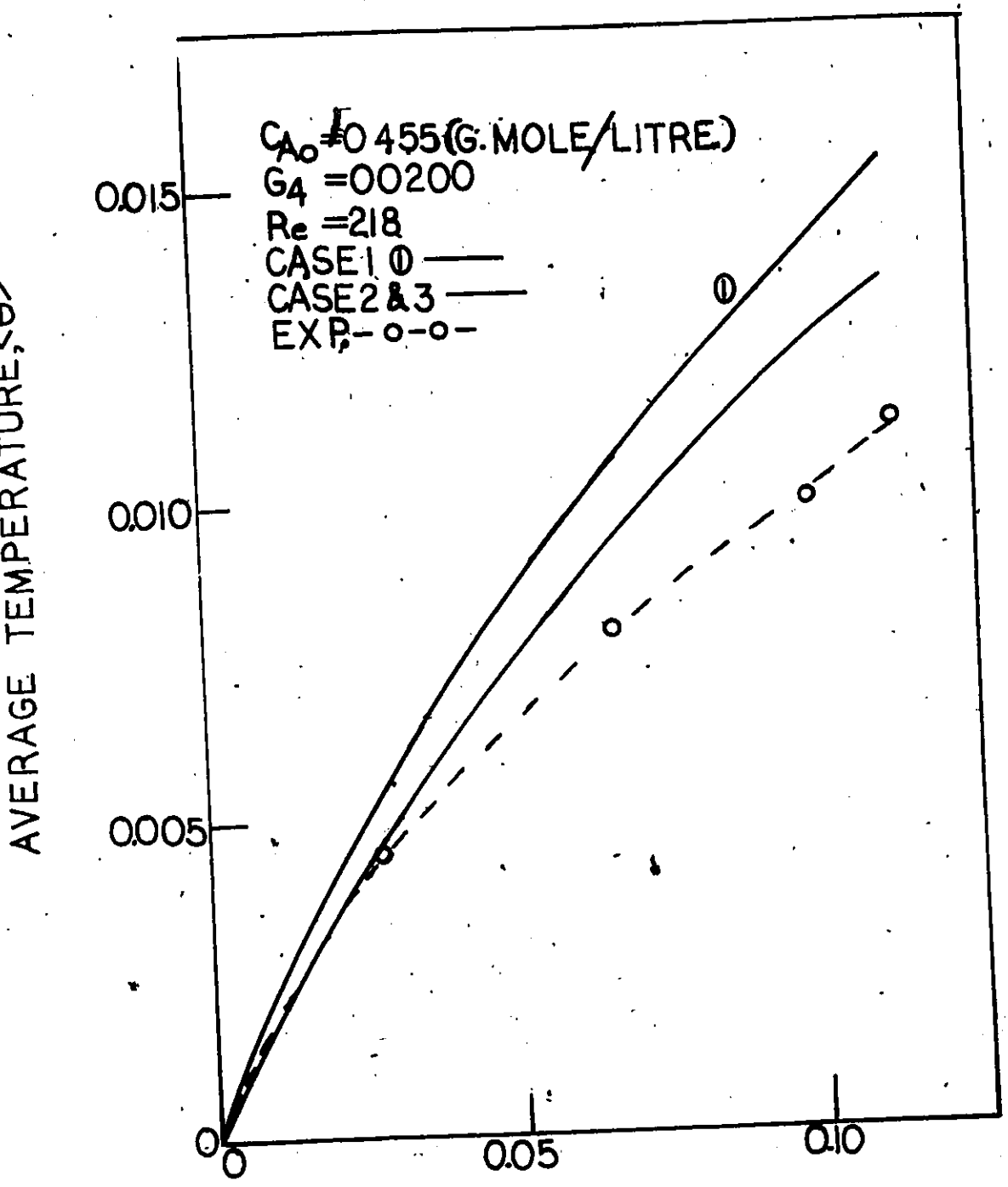
C_{A_0} = 0.455 (G. MOLE/LITRE.)
G_4 = 00200
Re = 218
CASE 1 ①
CASE 2 & 3
EXP. - o - o -
①
0.015
0.010
0.005
0
0
0.05
0.10
AVERAGE TEMPERATURE, <θ>
AXIAL DISTANCE, W

FIGURE-23

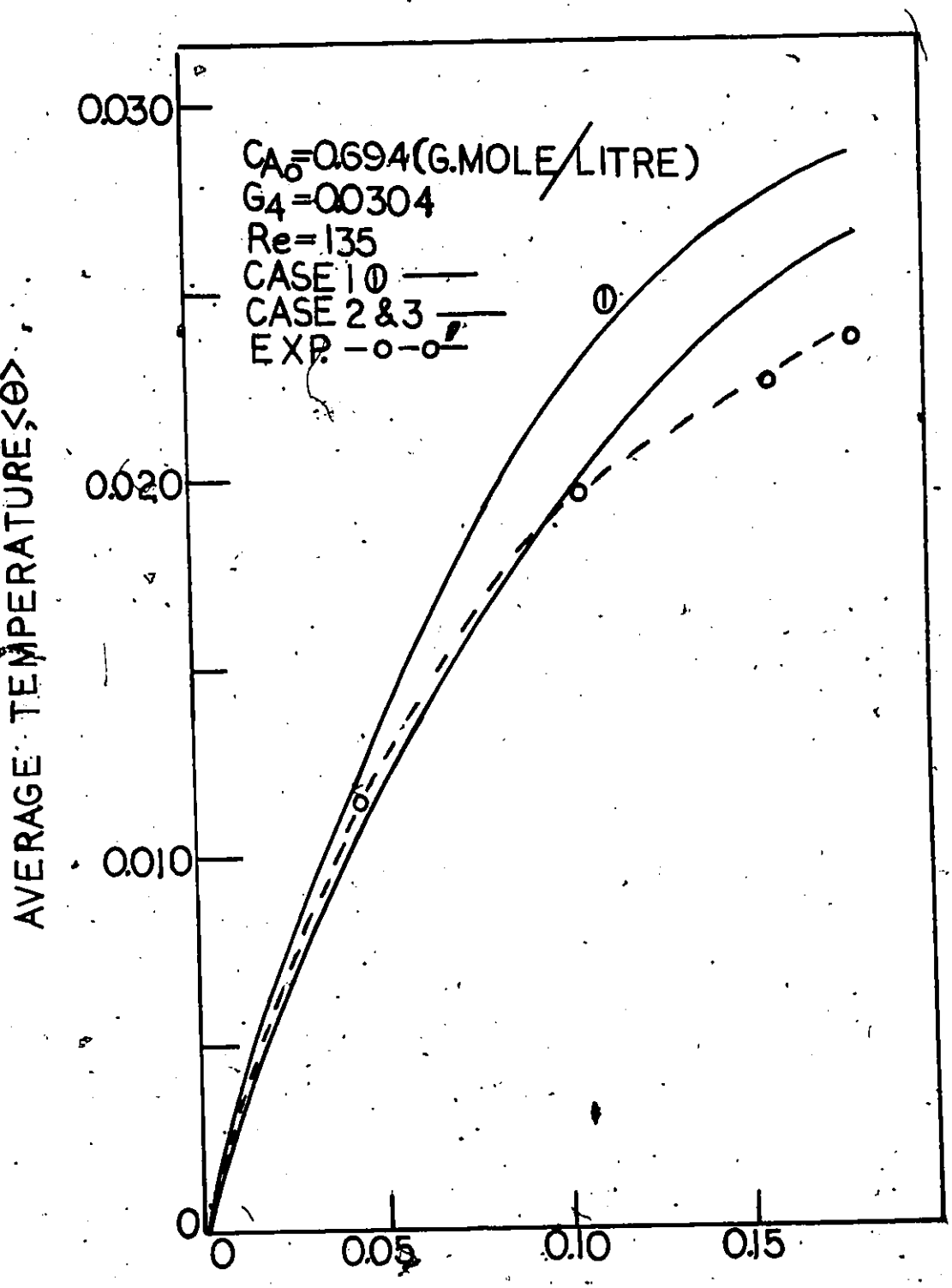
0.030
0.020
0.010
0
C_{A_0}=0.694(G.MOLE/LITRE)
G_4=0.0304
Re=135
CASE 1 ①
CASE 2 & 3
EXP. -o-o-
①
AVERAGE TEMPERATURE, <θ>
0
0.05
0.10
0.15
AXIAL DISTANCE, W

FIGURE-24

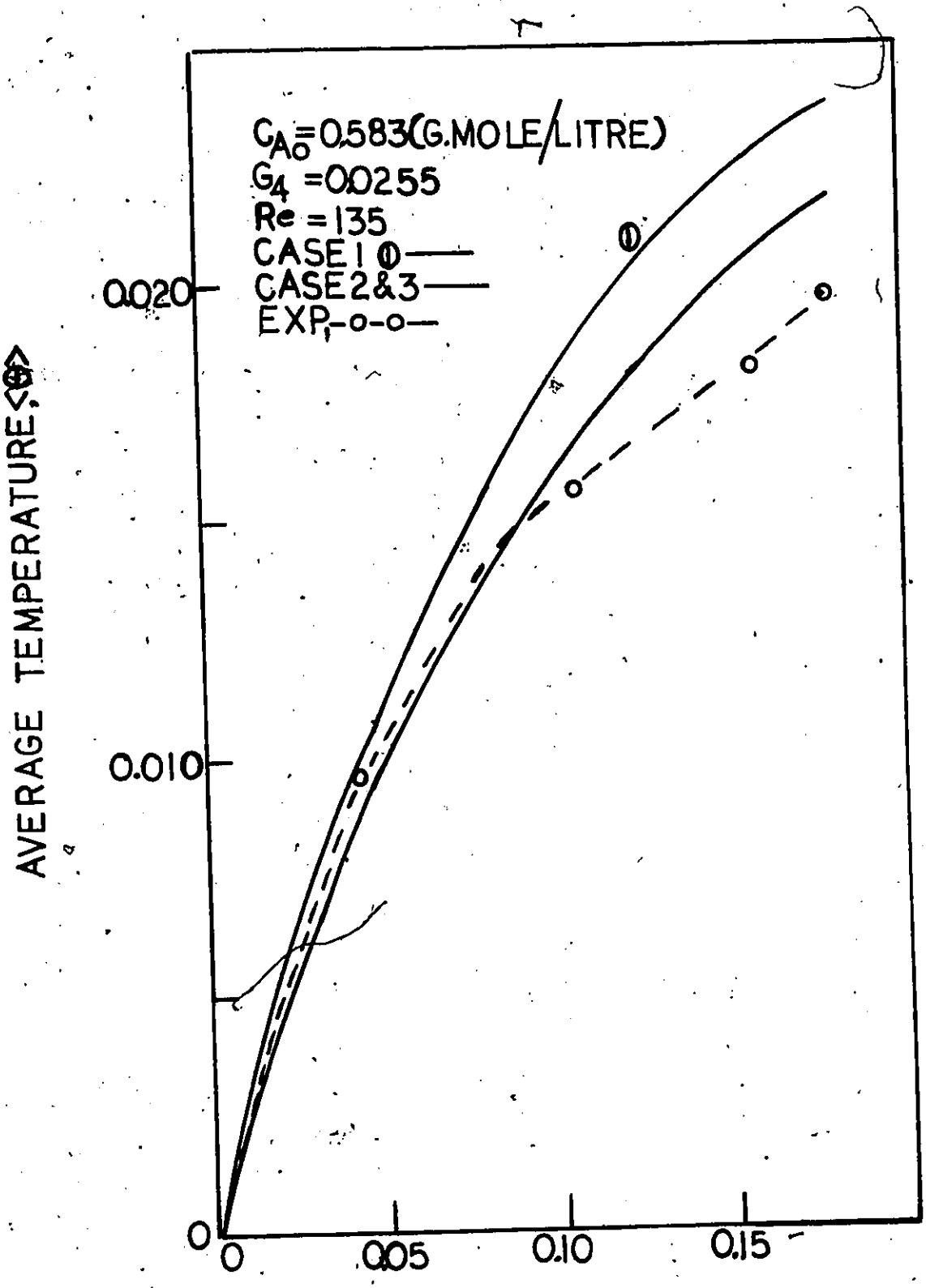
C_{A_0}=0.583(G.MOLE/LITRE)
G_4 =0.0255
Re =135
CASE1 ①——
CASE2&3——
EXP.-o-o—
①
0.020
0.010
0
0
0.05
0.10
0.15
AVERAGE TEMPERATURE, <θ>
AXIAL DISTANCE, W

FIGURE-25

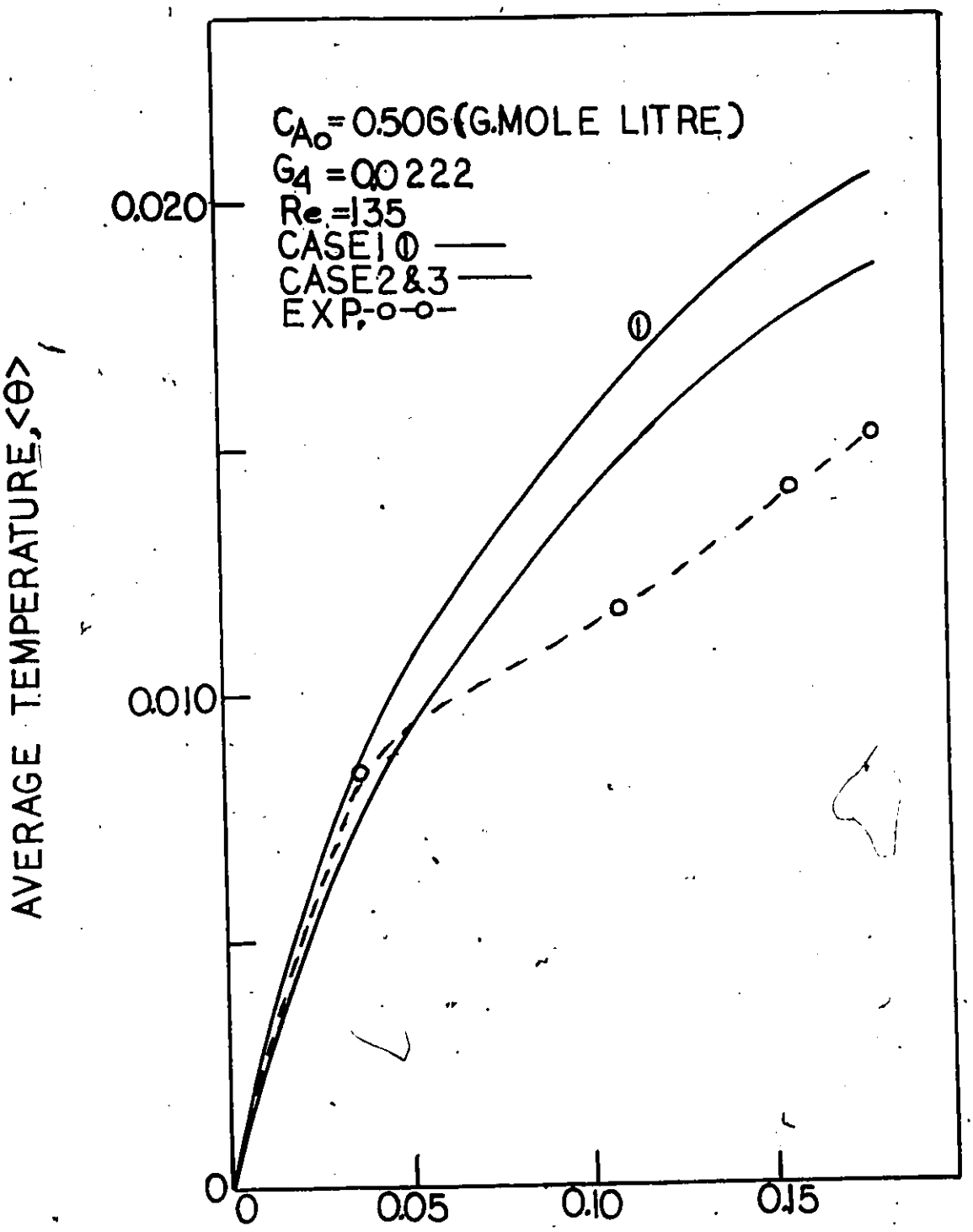
C_{A_0} = 0.506 (G.MOLE LITRE)
G_4 = 0.0222
Re. = 135
CASE 1 ①
CASE 2 & 3
EXP. -o-o-
①
0.020
0.010
0
0
0.05
0.10
0.15
AVERAGE TEMPERATURE, <θ>
AXIAL DISTANCE, W

FIGURE-26

As expected, the more uniform the velocity profile the greater the conversion. Figures 15 through 20 indicate that a lower average concentration x, was obtained in plug flow than in laminar flow. This difference became more significant as the residence time was decreased, as the following table shows.

			$\langle x \rangle$		
1.	w = 0.208	C_{A_o}	CASE 1	CASE 2	CASE 3
		0.694	0.039	0.105	0.104
		0.583	0.047	0.117	0.116
		0.506	0.054	0.126	0.125
	w = 0.129	0.706	0.154	0.251	0.250
		0.528	0.177	0.272	0.271
		0.455	0.187	0.281	0.280

TABLE -1

Also, the fraction of reactant unconverted $\langle x \rangle$, increased with decreasing inlet concentration. The average temperature $\langle \theta \rangle$ was also higher in plug flow as demonstrated in figures 21 to 26. As explained above, this was due to the greater conversion.

Agreement between the experimental results and the laminar flow model with radial diffusion(CASE 3) the model most closely representing the experimental system were generally poor. As can be seen from figures 3 through 8, the experimental radial profiles were flatter than theory predicted and at low axial distances, the experimental profiles intersected the theoretical profiles. At higher axial distances, they generally fell below the predicted values. Similarly, as shown in figures 21 to 26, the average experimental temperatures were in good agreement

at low axial distances but also fell below the theoretical values at higher axial distances.

The flat radial profiles and generally low experimental temperature values could be the result of the following factors:

1) the reactor was not operating adiabatically
2) the temperature probes were perpendicular to the flowing stream
3) natural convection

The first of these causes would not affect the reactor initially, because little heat is generated but would tend to have a pronounced effect at higher axial distances due to greater heat generation causing a correspondingly higher heat loss. As seen from figures 21 to 26, agreement with theoretically predicted values was much better at lower axial distances. The second reason would cause the temperatures read to represent average values rather than point values due to axial flow along the immersed length of the thermocouple probe. Lastly, natural convection in an adiabatic reactor, where the temperatures are for the most part higher at the wall than at the center would tend to flatten the velocity profile which in turn would tend to flatten the temperature profiles.

The experimental concentration profiles $\langle x \rangle$ were limited to inlet and outlet values of the reactor. For Re = 218, the outlet values agreed within 5% of the theoretical ones. For Re = 135, the outlet values were within 8% of those predicted by theory.

VI - CONCLUSIONS

(1) Theoretical average conversions and temperatures were greater in plug flow than in laminar flow. In general, conversions decreased with increasing Reynolds Number.

(2) Theoretical concentration and temperature profiles for both laminar flow models were nearly identical. Thus, diffusion had little effect on the system investigated.

(3) Also for the laminar flow models:

a) the concentration profiles decreased from the center to the wall and flattened out at higher axial distances.

b) the temperature profiles initially exhibited a maximum at the wall which shifted towards the centre as the reaction proceeded.

(4) The experimental radial temperature profiles were generally flatter than the theoretically predicted ones. Average temperatures showed better agreement at lower axial distances.

VII - RECOMMENDATIONS

Solutions to both laminar flow models could not be properly compared with the experimental results. The following modifications to the apparatus may provide a better comparison:

1) the thermocouple probes could be bent parallel to the flow of reactants.
2) the internal diameter of the reactor could be reduced

The analysis could also be expanded to include solutions for a reactor operating with a constant wall temperature.

REFERENCES

(1) F.A. Cleland and R.H. Wilhelm, "Diffusion and Reaction in a Viscous-Flow Tubular Reactor", A.I.Ch.E. Journal, 2, 489 (1956).

(2) J.P. Vignes and P.J. Trambauze, "Diffusion and Chemical Reaction in a Laminar-Flow Tubular Reactor", Chem. Eng. Sci., 17, 73 (1962).

(3) P.L. Chambré, "On Chemical Reactions in Internal Flow Systems", Appl. Sci. Res., A9, 157 (1960).

(4) J.P. Irving and J.M. Smith, "Heat Transfer in a Chemically Reacting System (Nitrogen Tetroxide-Dioxide)", A.I.Ch. E. Journal, 7, 91 (1961).

(5) K.G. Denbigh, "Chemical Reactor Theory", Vol. 1, Chap. 2, Cambridge University Press (1965).

(6) J.F. Wehner and R.H. Wilhelm, "Boundary Conditions of Flow Reactor", Chem. Eng. Sci., 6, 89 (1956).

(7) R.I. Rothenberg and J.M. Smith, "Dissociation and Heat Transfer in Laminar Flow", Can. J. Chem. Eng., 44, 67 (1966).

(8) R.I. Rothenberg and J.M. Smith, "Heat Transfer and Reaction in Laminar Flow", A.I.Ch.E. Journal, 16, 542 (1970).

(9) R.B. Bird, W.E., Stewart and E.N. Lightfoot, "Transport Phenomena", John Wiley and Sons, New York (1960).

(10) L.S. Merril, Jr. and C.E. Hamrin, Jr., "Conversions and Temperature Profiles for Complex Reactions in Laminar and Plug Flow", A.I.Ch.E. Journal, 16, 194 (1970).

(11) V.G. Jensen and G.V. Jeffreys, "Mathematical Methods in Chemical Engineering", p. 420. Academic Press, New York (1963).

(12) R.C.L. Bosworth, Phil. Mag., 39, No. 7, 847 (1948).

(13) M. L. Trombetta and J. Happel, "Analysis and Design of Gas Flow Reactors with Applications to Hydrocarbon Pyrolysis", A.I.Ch.E. Journal, 11, 1041(1965).

(14) T.S. Andersen and J. Coull , "Evaluation of Models for Tubular, Laminar Flow Reactors", A.I.Ch.E. Journal, 16, 542 (1970).

(15) L. Lapidus, "Digital Computation for Chemical Engineers", Chap 4. McGraw Hill, New York (1962).

(16) Handbook of Chemistry and Physics, p. 1766, 30th ed., (1947).

(17) International Critical Tables", p. 114-115, Volume V.

(18) Handbook of Chemistry and Physics, p. 1791, 30th ed., (1947).

(19) Handbook of Chemistry and Physics, p. 594, 30th ed., (1947).

(20) Handbook of Chemistry and Physics, p. 1695, 30th ed., (1947).

(21) Internationa Critical Tables, p. 123, Volume III.

(22) B.C. Sakiadis and J. Coates, "A Literature Survey of the Thermal Conductivities of Liquids", Eng. Expt. Sta. Bull. 34, Louisana State University, Baton Rouge, La, (1952). .

(23) E.F.M. Van Der Held and F.G. Van Dreeven: Physica, 15 , 865 (1949).

(24) P.A. Johnson and A.L. Babb, Chem. Revs., 56, 387 (1956).

(25) J.F.M. Caudri, "The Velocity of Hydrolysis and Alcoholysis of Acetic Anhydride in Mixtures of Water and Ethyl or Methyl Alcohol", Rec. Tran. Chim., 49, 1 (1930).

(26) S. E. Vles, "The Determination of the Velocity of Hydrolysis of Acid Anhydrides by the Aniline-Water Method", Rec. Trav. Chim., 52, 809 (1933).

APPENDICES

APPENDIX A

EXPERIMENTAL DATA

1. Radial Temperature Traverses

The thermocouple probe axial positions as measured from the end of the inlet conical section of the reactor were:

TC 1	35 cm
TC2	100 cm
TC3	163 cm
TC4	191 cm

The radial positions were measured from one wall of the reactor to the centre line and from the opposite wall again to the centre line.

TEST RUN 1A

Inlet Concentration of Acetic Anhydride = 0.706 (g.mole)/litre
Reynolds Number = 218
Inlet Temperature = 29.2 (°C)

TC Position	TC1 (MV)	TC1 (°C)	TC2 (MV)	TC2 (°C)	TC3 (MV)	TC3 (°C)	TC4 (MV)	TC4 (°C)
$Wall_1$	1.389	35.24	1.346	34.20	1.321	33.60	1.236	31.55
1/16	1.393	35.34	1.360	34.54	1.329	33.79	1.245	31.76
2/16	1.400	35.51	1.380	35.03	1.333	33.89	1.254	31.98
3/16	1.411	35.77	1.390	35.27	1.330	33.82	1.253	31.96
3/8	1.416	35.89	1.392	35.31	1.324	33.67	1.234	31.50
4/8	1.401	35.53	1.383	35.10	1.321	33.60	1.227	31.33
5/8	1.394	35.36	1.385	35.15	1.320	33.58	1.227	31.33
11/16 (CL)	1.391	35.29	1.386	35.17	1.320	33.58	1.225	31.28
5/8	1.396	35.41	1.383	35.10	1.314	33.43	1.225	31.28
4/8	1.401	35.53	1.389	35.24	1.321	33.60	1.227	31.33
3/8	1.399	35.48	1.390	35.27	1.328	33.77	1.229	31.38
3/16	1.411	35.77	1.394	35.36	1.332	33.87	1.236	31.55
2/16	1.411	35.77	1.392	35.31	1.344	34.16	1.246	31.79
1/16	1.410	35.75	1.394	35.36	1.343	34.13	1.247	31.81
$Wall_2$	1.409	35.73	1.395	35.39	1.343	34.13	1.250	31.89

TABLE A1-1

TEST RUN 2A

Inlet Concentration of Acetic Anhydride = 0.529 ($\frac{\text{g. mole}}{\text{litre}}$)
Reynolds Number = 218
Inlet Temperature = 29.2 (°C)

TC Position	TC1 (MV)	TC1 (°C)	TC2 (MV)	TC2 (°C)	TC3 (MV)	TC3 (°C)	TC4 (MV)	TC4 (°C)
$Wall_1$	1.313	33.41	1.291	32.88	1.280	32.61	1.216	31.06
1/16"	1.324	33.67	1.306	33.24	1.285	32.73	1.231	31.43
2/16"	1.332	33.87	1.320	33.58	1.297	33.02	1.231	31.43
3/16"	1.337	33.98	1.328	33.77	1.299	33.07	1.231	31.43
3/8"	1.343	34.13	1.331	33.84	1.288	32.80	1.221	31.19
4/8"	1.336	33.96	1.327	33.75	1.283	32.68	1.214	31.02
5/8"	1.330	33.82	1.324	33.67	1.275	32.49	1.207	30.85
11/16 (CL)	1.325	33.70	1.318	33.53	1.275	32.49	1.204	30.77
5/8"	1.330	33.82	1.321	33.60	1.275	32.49	1.210	30.92
4/8"	1.336	33.96	1.324	33.67	1.277	32.54	1.214	31.02
3/8"	1.338	34.01	1.321	33.60	1.279	32.59	1.211	30.94
3/16"	1.336	33.96	1.327	33.75	1.290	32.85	1.222	31.21
2/16"	1.340	34.06	1.333	33.89	1.290	32.85	1.234	31.50
1/16"	1.345	34.18	1.334	33.91	1.295	32.97	1.231	31.43
$Wall_2$	1.345	34.18	1.332	33.87	1.292	32.90	1.235	31.52

TABLE A1-2

TEST RUN 3A

Inlet Concentration of Acetic Anhydride = 0.455 ($\frac{\text{g. mole}}{\text{litre}}$)
Reynolds Number = 218.
Inlet Temperature = 29.2 (°C)

TC Position	TC1 (MV)	TC1 (°C)	TC2 (MV)	TC2 (°C)	TC3 (MV)	TC3 (°C)	TC4 (MV)	TC4 (°C)
$Wall_1$	1.264	32.22	1.241	31.67	1.236	31.55	1.183	30.27
1/16"	1.267	32.30	1.252	31.93	1.242	31.69	1.201	30.70
2/16"	1.279	32.59	1.264	32.22	1.246	31.79	1.205	30.80
3/16"	1.282	32.66	1.274	32.47	1.252	31.93	1.200	30.68
3/8"	1.284	32.71	1.276	32.51	1.237	31.57	1.193	30.51
4/8"	1.276	32.51	1.270	32.37	1.235	31.52	1.186	30.34
5/8"	1.279	32.59	1.266	32.27	1.230	31.40	1.185	30.32
11/16 (CL)	1.279	32.59	1.264	32.22	1.226	31.31	1.181	30.22
5/8"	1.279	32.59	1.270	32.37	1.230	31.40	1.184	30.29
4/8"	1.279	32.59	1.267	32.30	1.234	31.50	1.189	30.41
3/8"	1.283	32.68	1.270	32.37	1.239	31.62	1.188	30.39
3/16"	1.285	32.73	1.270	32.37	1.242	31.69	1.191	30.46
2/16"	1.284	32.71	1.274	32.47	1.240	31.64	1.193	30.51
1/16"	1.285	32.73	1.275	32.49	1.245	31.76	1.194	30.53
$Wall_2$	1.280	32.61	1.276	32.51	1.249	31.86	1.196	30.58

TABLE A1-3

TEST RUN 1B

Inlet Concentration of Acetic Anhydride = 0.694 ($\frac{\text{g. mole}}{\text{litre}}$)
Reynolds Number = 135
Inlet Temperature = 29.2 (°C)

TC Position	TC1 (MV)	TC1 (°C)	TC2 (MV)	TC2 (°C)	TC3 (MV)	TC3 (°C)	TC4 (MV)	TC4 (°C)
$Wall_1$	1.407	35.68	1.387	35.19	1.359	34.52	1.270	32.37
1/16"	1.419	35.97	1.398	35.46	1.370	34.78	1.282	32.66
2/16"	1.429	36.21	1.414	35.85	1.385	35.15	1.296	33.00
3/16"	1.435	36.35	1.424	36.09	1.385	35.15	1.298	33.04
3/8"	1.437	36.40	1.430	36.23	1.375	34.90	1.275	32.49
4/8"	1.436	36.38	1.424	36.09	1.372	34.83	1.268	32.32
5/8"	1.434	36.33	1.419	35.97	1.374	34.88	1.275	32.49
11/16" (CL)	1.435	36.35	1.417	35.92	1.374	34.88	1.266	32.27
5/8"	1.436	36.38	1.424	36.09	1.373	34.86	1.266	32.27
4/8"	1.436	36.38	1.424	36.09	1.370	34.78	1.270	32.37
3/8"	1.438	36.43	1.425	36.11	1.373	34.86	1.277	32.54
3/16"	1.440	36.47	1.429	36.21	1.382	35.07	1.276	32.51
2/16"	1.439	36.45	1.430	36.23	1.385	35.15	1.285	32.73
1/16"	1.437	36.40	1.429	36.21	1.387	35.20	1.286	32.76
$Wall_2$	1.434	36.33	1.429	36.21	1.380	35.03	1.291	32.88

TABLE A1-4

TEST RUN 2B

Inlet Concentration of Acetic Anhydride = 0.583 ($\frac{\text{g. mole}}{\text{litre}}$)
Reynolds Number = 135
Inlet Temperature = 29.2 (°C)

TC Position	TC1 (MV)	TC1 (°C)	TC2 (MV)	TC2 (°C)	TC3 (MV)	TC3 (°C)	TC4 (MV)	TC4 (°C)
$Wall_1$	1.370	34.78	1.340	34.06	1.320	33.58	1.256	32.03
1/16"	1.378	34.98	1.350	34.30	1.327	33.75	1.264	32.22
2/16"	1.385	35.15	1.364	34.64	1.335	33.94	1.270	32.37
3/16"	1.385	35.15	1.374	34.88	1.344	34.16	1.274	32.47
3/8"	1.387	35.19	1.372	34.83	1.339	34.04	1.260	32.13
4/8"	1.389	35.24	1.370	34.78	1.325	33.70	1.248	31.84
5/8"	1.386	35.17	1.370	34.78	1.320	33.58	1.245	31.76
11/16" (CL)	1.386	35.17	1.369	34.76	1.316	33.48	1.243	31.72
5/8"	1.383	35.10	1.365	34.66	1.325	33.70	1.251	31.91
4/8"	1.386	35.17	1.366	34.69	1.330	33.82	1.262	32.18
3/8"	1.384	35.12	1.369	34.76	1.336	33.96	1.264	32.22
3/16"	1.390	35.27	1.370	34.78	1.346	34.20	1.269	32.34
2/16"	1.388	35.22	1.376	34.93	1.355	34.42	1.270	32.37
1/16"	1.389	35.24	1.375	34.90	1.354	34.40	1.276	32.51
$Wall_2$	1.382	35.07	1.374	34.88	1.355	34.42	1.276	32.51

TABLE A1-5

TEST RUN 3B

Inlet Concentration of Acetic Anhydride = 0.506 ($\frac{\text{g. mole}}{\text{litre}}$)
Reynolds Number = 135
Inlet Temperature = 29.2 (°C)

TC Position	TC1 (MV)	TC1 (°C)	TC2 (MV)	TC2 (°C)	TC3 (MV)	TC3 (°C)	TC4 (MV)	TC4 (°C)
$Wall_1$	1.305	33.21	1.284	32.71	1.272	32.42	1.246	31.79
1/16"	1.315	33.46	1.299	33.07	1.280	32.61	1.255	32.01
2/16"	1.323	33.65	1.310	33.33	1.287	32.78	1.256	32.03
3/16"	1.326	33.72	1.317	33.50	1.290	32.85	1.261	32.15
3/8"	1.331	33.84	1.320	33.57	1.288	32.80	1.247	31.81
4/8"	1.330	33.82	1.319	33.55	1.280	32.61	1.235	31.52
5/8"	1.320	33.82	1.319	33.55	1.275	32.49	1.231	31.43
11/16"(CL)	1.329	33.79	1.314	33.43	1.275	32.49	1.233	31.48
5/8"	1.327	33.75	1.315	33.46	1.273	32.44	1.235	31.52
4/8"	1.325	33.70	1.319	33.55	1.278	32.56	1.238	31.60
3/8"	1.329	33.79	1.321	33.60	1.280	32.61	1.241	31.67
3/16"	1.331	33.84	1.326	33.72	1.281	32.63	1.246	31.79
2/16"	1.331	33.84	1.325	33.70	1.281	32.63	1.251	31.91
1/16"	1.330	33.82	1.323	33.65	1.291	32.88	1.251	31.91
$Wall_2$	1.330	33.82	1.320	33.58	1.291	32.88	1.253	31.96

TABLE A1-6

2. Concentration

The concentration of acetic anhydride was measured at the inlet and outlet of the reactor. For details of the method used, see Appendix C.

Run Number	Inlet Concentration (g. mole/litre)	Outlet Concentration (g. mole/litre)
1A	0.706	0.155
2A	0.528	0.133
3A	0.455	0.134
1B	0.694	0.080
2B	0.583	0.076
3B	0.506	0.126

TABLE A2-1

3. Flow Rate

The volumetric flow rate was obtained by measuring the time required to collect 2 litres of effluent solution at the reactor exit.

Run Number	Volume Collected (l.)	Time (sec)	Volumetric Flow Rate (ml/sec)
1A	2	440	4.54
2A	2	441	4.53
3A	2	438	4.56
1B	2	712	2.82
2B	2	712	2.82
3B	2	711	2.82

TABLE A3-1

APPENDIX B

KINETIC DATA AND PHYSICAL PROPERTIES

1. Estimation of the Frequency Factor (A_I), and the Energy of Activation (E)

The hydration of acetic anhydride is a well studied reaction with known first-order kinetics[1, 25, 26]. Values of the reaction rate constant reported in the literature are shown below.

Concentration (g. mole/l.)	Temperature (°C)	Reaction Rate constant (min^{-1})
0.490	0°C	0.023
0.495	0°C	0.028
0.473	15°C	0.074
0.3389	18°C	0.0916
0.4872	25°C	0.1384
0.5352	25°C	0.1328

TABLE B1-1

From the Arrhenius equation, the reaction rate constant can be expressed as

$$k_I = A_I \exp\left(\frac{-E}{RT}\right) \qquad (B-1)$$

or alternately

$$\ln k_I = \ln A_I - \frac{E}{RT} \qquad (B-2)$$

A least squares fit on the reported data gave

$$\ln k_I = \frac{-5,352.9}{T} + 15.946 \qquad \text{(B-3)}$$

such that the frequency factor is given by

$$A_o = 0.841898 \times 10^7 \ (\text{min}^{-1})$$

and the activation energy by

$$E = 10,636.2 \ (\text{cal/g. mole}).$$

2. Physical Properties

a) Heat Capacity (C_p)

Litterature values were not available for the heat capacity of acetic anhydride and it was estimated by the method suggested by Sakiadis and Coates[22]. The values for water and acetic acid were taken from the references indicated.

Temperature (°C)	C_p (cal./g.-°C) Acetic Anhydride	Water[16]	Acetic Acid[17]
29	0.383	0.99804	0.495
30		0.99802	0.496
31		0.99799	0.497
32	0.387	0.99797	0.498
33		0.99797	0.499
34		0.99795	0.500
35	0.391	0.99795	0.501
36		0.99797	0.502

TABLE B2-1

b) Density (ρ)

The density of acetic anhydride[19] has a value of 1.08 (g./ml.). The values for water and acetic acid are tabulated below.

Temperature (°C)	ρ (g. ml.) Water[20]	Acetic Acid[16]
29	0.9960	1.0356
30	0.9957	1.0354
31	0.9954	1.0343
32	0.9951	1.0331
33	0.9947	1.0318
34	0.9944	1.0315
35	0.9941	1.0292
36	0.9937	1.0280

TABLE B2-2

c) Thermal Conductivity (k_c)

	k_c (cal/cm-°C-sec)
Acetic Anhydride [16]	0.00033
Water [16]	0.00148
Acetic Acid [16, 17]	0.00093

TABLE B2-3

d) Diffusion Coefficient (D_A)

The diffusion coefficient of acetic anhydride was estimated by the method of Othmer and Thakar[18] and is given by

$$D_A = \frac{14.0 \times 10^{-5}}{\mu_w^{1.1} V_1^{0.6}} \qquad (B-4)$$

where μ_w = viscosity of water in centipoise

V_1 = molal volume of solute in cc/g.mole

The table below summarizes the values obtained

Temperature (°C)	$D_A \times 10^{-5}$ (cm^2/sec)
29	1.0623
30	1.0887
31	1.1142
32	1.1480
33	1.1660
34	1.1925
35	1.2191
36	1.2456

TABLE B2-4

3. Physical Properties of Reacting Mixture

The physical properties of the reacting mixture were calculated on a mole fraction basis from the average values of the individual species of the mixture. Calculations were made at the inlet and outlet conditions for each run. In each case, the values obtained were nearly identical and the average values are shown below.

$$C_{p_{mix}} = 0.984 \text{ (cal/g.mole - °C)}$$

$$\rho_{mix} = 1.001 \text{ (g./ml.)}$$

$$k_{C_{mix}} = 0.00147 \text{ (cal/cm - °C - sec)}$$

APPENDIX C

CONCENTRATION ANALYSIS

The inlet and outlet concentration were measured by the aniline-water method[24,25]. The method consisted of catching two samples into tared flasks, one of which contained ten to fifteeen times the amount of saturated aniline-water needed to react completely with the acetic anhydride. The reaction proceeds very rapidly and forms acetanilide, a non-titratable compound. The other was left to hydrolyse completely. The flasks were then reweighed and the solutions titrated with caustic soda by use of a phenophthalein indicator.

If A indicated the concentration of acetic anhydride at the sampling point, and x the amount of acetic acid already present, then the amount of acid present in the completely hydrolysed sample would be 2A + x.

$$(CH_3\,CO)_2\,O + H_2O = 2\,CH_3\,COOH$$

A	x	sampling point
O	2A + x	time = ∞

When the reaction is stopped by the aniline-water mixture the amount of acid present is A + x.

$$(CH_3\,CO)_2 + H_2O = 2\,CH_3\,COOH$$

A	x sampling point

$$(CH_3\,CO)_2 + C_6H_5NH_2 = CH_3\,COOH + C_6H_5NHCOCH_3$$

A	A

$$\text{Total acid} = \frac{A}{A + x}$$

Knowing the acid content of the two samples gives the acetic anhydride concentration at the sampling point, that is

$$(2A + x) - (A + x) = A.$$

The titrations were carried out with caustic soda which was standardized against potassium acid phthalate.

APPENDIX D

EQUIPMENT SPECIFICATIONS

1. Pump:

   Manufacturer: Milli Royal

   Model: Duplex D4 117 and Mo DO 117

   Specifications: Both sides positive displacement
   Rated: 1000 psi

2. Millivolt Potentiometer

   Manufacturer: Leeds and Northrup

   Model: 8686 Millivolt Potentiometer

   Specifications: Scale: 1 to 10 m.v. $\pm$ 0.00025 m.v.

APPENDIX E

CALIBRATION CHARTS

1. Thermocouple Probes

The thermocouple probes were calibrated with a Beckman thermometer. The calibration curves were the same for all the thermocouples used and only one is shown in figure 27.

2. Pump

The pump was calibrated by noting the time required to collect a sample in a tared flask and weighing. The calibration curves for the water and acetic anhydride side of the pump are shown in figure 28.

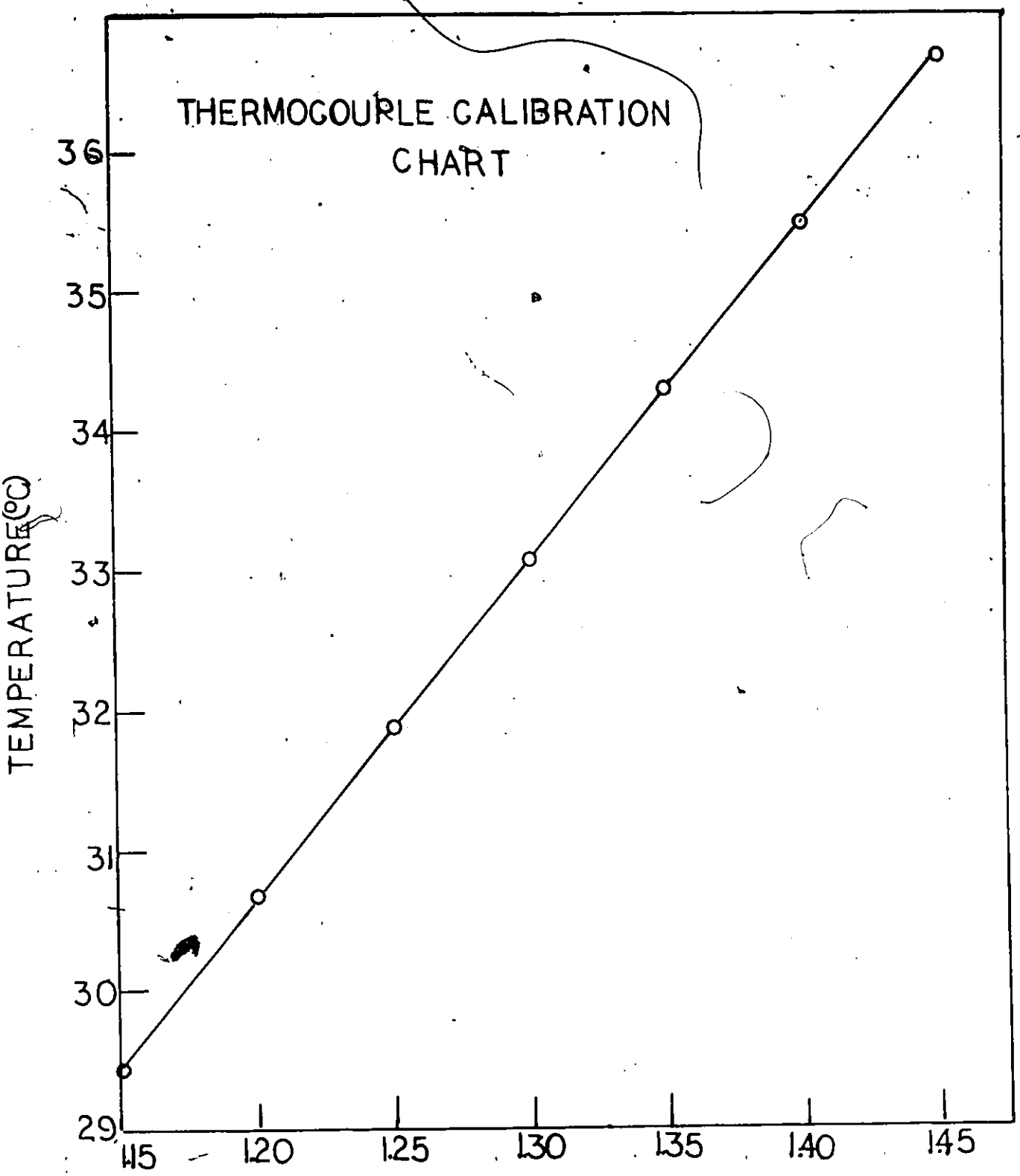
THERMOCOUPLE CALIBRATION CHART
TEMPERATURE (°C)
36
35
34
33
32
31
30
29
1.15
1.20
1.25
1.30
1.35
1.40
1.45
MILLIVOLTS

FIGURE-27

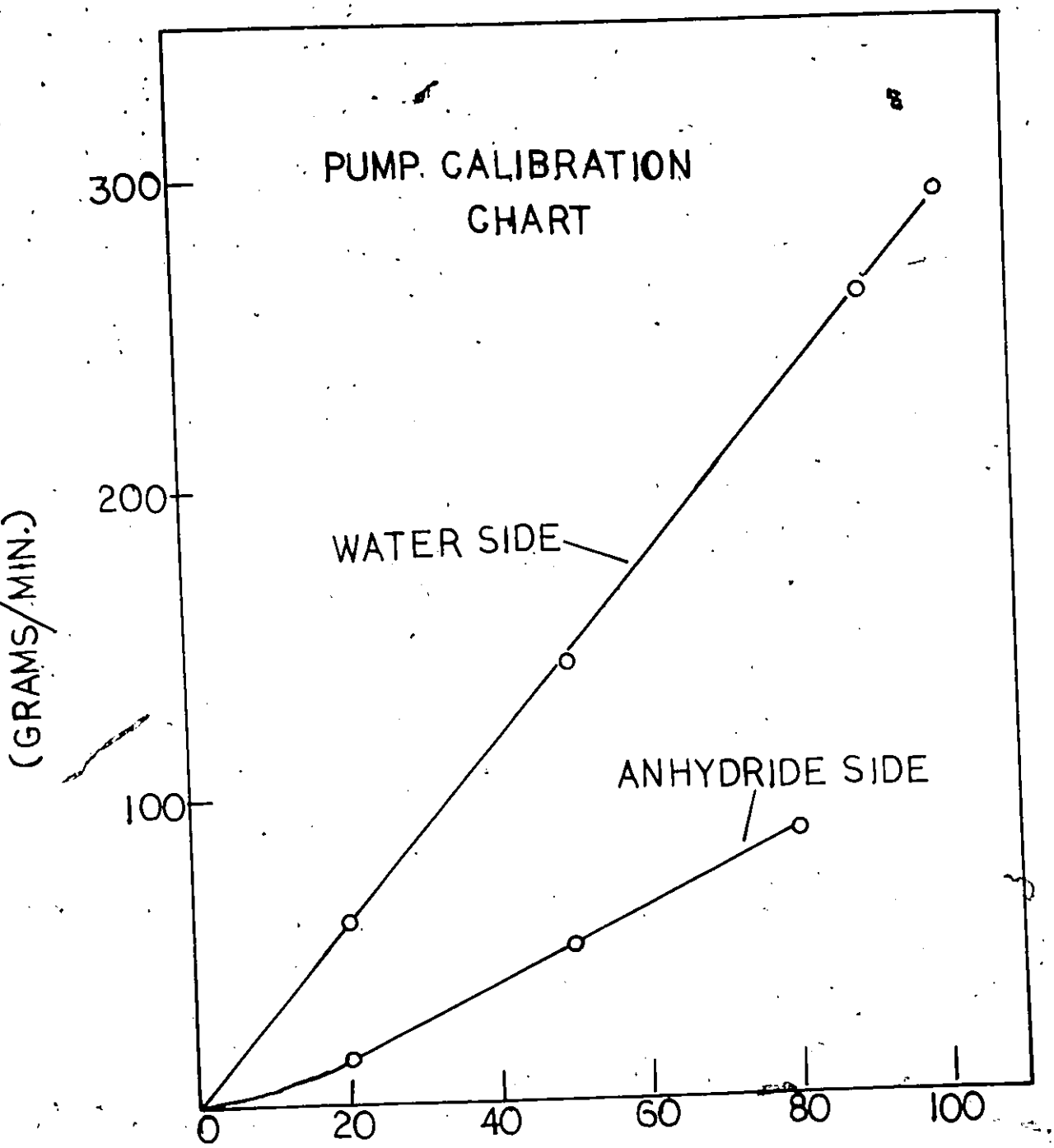
PUMP. CALIBRATION
CHART
300
200
100
(GRAMS/MIN.)
WATER SIDE
ANHYDRIDE SIDE
0
20
40
60
80
100
PUMP SETTING(%)

FIGURE-28

APPENDIX F

COMPUTER PROGRAM

The system of linear simultaneous equations derived from the finite difference approximations were solved by machine computation. A basic Gauss-elimination subroutine package was used. The programs for the solution of the three cases were basically similar and only Case 3 is presented here.

```
      DIMENSION X(11,120),THETA(11,120),P(11,1),A(11,11),AA(11),FUNC1(11
     1),FUNC2(11),TCEL(11,120),CONC(11),THETAC(11)
      DIMENSION AX(11,11),RX(11,1)
      DIMENSION AR(11),XAL(11),VX(11,11),RVX(11,11),ASTD(11)
C
C     THIS IS CASE III
C
C     FINITE DIFFERENCE PROGRAM
C     ADIABATIC REACTOR
      REAL KC
C     CONSTANTS
C
C     INITIAL TEMPERATURE IN DEGREES KELVIN
  630 READ(1,631) VF,CAO
  631 FORMAT(2F10.0)
      RO=1.746
      RI=0.238
      B=28./10.
      AKR=(1.1836/60.
C     TO CALCULATE RADIAL AND AXIAL VELOCITY PROFILES USING LAMINAR FLOW
C     HYPOTHESIS
      DO 20 I=1,11
      D=I
      AR(I)=RI+(D-1.)/10.*(RO-RI)
      XAL(I)=3.1416*AR(I)*AR(I)
      DO 20 J=1,11
      Y=J
      VX(I,J)=2.*VF/XAL(I)*(1.-((Y-1.)*(Y-1.)/100.))
      IF(VX(I,J).EQ.0.0)VX(I,J)=(2.*VF/XAL(I))/10.
   20 RVX(I,J)=1.0/VX(I,J)
C     USE OF SIMPSON'S RULE TO CALCULATE TIME DISTRIBUTION IN AXIAL
C     DIRECTION
      DO 30 I=1,11
      ASTD(I)=0.0
      DO 30 K=2,10,2
   30 ASTD(I)=(B/3.)*(RVX(K-1,I)+4.*RVX(K,I)+RVX(K+1,I))+ASTD(I)
C     CONCENTRATION AND TEMPERATURE PROFILES FOUND USING FIRST ORDER
C     KINETICS
      H2OV=((1000.-(CAO*102.*(1./1.08))/18.)*17.96
      DO 40 I=1,11
      CONC(I)=CAO*EXP(-AKR*ASTD(I))
      THETAC(I)=29.2+((13.6)*(CAO-CONC(I)))/(H2OV+2.33*(CAO-CONC(I))))
   40 CONTINUE
      TI=5.30235E03
      AN=6.140316E06
      H = .1
      GH=.1
      SOUT = 10.0E-06
C     VALUES OF ARRAY AA
      AA(1) = 0.0
      DO 37 IJ = 2,11
   37 AA(IJ) = AA(IJ-1)+.1
      F=1.636.2
      RC = 1.987
      KC=3.0.147
      ROW=1.
      CP= .384
```

```
                      DA=.0000001157
                      G1=(CP*ROW*DA)/KC
                      G2=E/(RC*TI)
                      G3=(RO**O*ROW*CP*AO)/KC
                      GB=(DELTAH*CAO)/(TI*ROW*CP)
                      G4=GB/1000.
                      Z=221.
                      VELOX=VF/(3.14   *RO*RO)
                      W=(KC*Z)/(3.   *RO*RO*VELOX*ROW*CP)
                      GK=W/110.
                      WRITE(3,606)
                  606 FORMAT(1H1,T30,'THE VALUES OF THE ROTHENBERG DIMENSIONLESS PARAMET
                     1ERS ARE:',////)
                      WRITE(3,607) G1,G2,G3,G4
                  607 FORMAT(T2,'G1=',E14.9,T30,'G2=',E14.9,T60,'G3=',E14.9,T90,'G4=',E1
                     14.9,//)
                      WRITE(3,608) VF,W,CAO
                  608 FORMAT(T2,'VF=',F10.5,T30,'W=',F10.5,T60,'CAO=',F10.5,//)
                      AREA1 = 0.0
                      AREA2 = 0.0
                      DO 70 IX=1,11
                      X(IX,1)=(CONC(IX)/CAO
                      THETA(IX,1)=((THETAC(IX)+273.15)-TI)/TI
                      FUNC1(IX)=X(IX,1)*AA(IX)*(1.0-AA(IX)*AA(IX))
                   70 FUNC2(IX)=THETA(IX,1)*AA(IX)*(1.0-AA(IX)*AA(IX))
                      DO 42 JI=2,10,2
                      AREA1 = AREA1+((H/3.0)*(FUNC1(JI-1)+(4.0*FUNC1(JI))+FUNC1(JI+1)))
                      AREA2 = AREA2+((H/3.0)*(FUNC2(JI-1)+(4.0*FUNC2(JI))+FUNC2(JI+1)))
                   42 CONTINUE
                      AVTEMP = 4.0*AREA2
                      AVCONS = 4.0*AREA1
                      WRITE(3,200) AVCONS,AVTEMP
                  200 FORMAT(1H1,T30,'AVERAGE CONTRETATION',F16.7,//,T30,'AVERAGE TEMPER
                     1ATURE',E16.7)
                      ICOUNT = 1
                      N = 1
                    2 ICOUNT = ICOUNT+1
                      AREA1 = 0.0
                      AREA2 = 0.0
                      DO 21 MA = 1,11
                      DO 21 NA = 1,11
                   21 AX(MA,NA) = 0.0
                      AX(1,1) = 1.0+((2.0*GK*G1)/(GH*GH))+(GK*(G3/2.0)*EXP(-G2/(THETA(1,
                     1N)+1.0)))
                      AX(1,2) = -(2.0)*GK*G1)/(GH*GH)
                      DO 22 IMA = 2,10
                      AX(IMA,IMA-1) = (GK*G1*(GH-2.0*AA(IMA)))/(4.0*AA(IMA)*GH*GH*(1.0-A
                     1A(IMA)*AA(IMA)))
                   22 CONTINUE
                      DO 23 KMA = 2,10
                      AX(KMA,KMA) = 1.0+((GK*G1)/(GH*GH*(1.0-AA(KMA)*AA(KMA))))+((GK*G3*
                     1EXP(-G2/(THETA(KMA,N)+1.0)))/(2.0*(1.0-AA(KMA)*AA(KMA))))
                   23 CONTINUE
                      DO 24 JMA = 2,10
                      AX(JMA,JMA+1) = -(GK*G1*(GH+2.0*AA(JMA)))/(4.0*AA(JMA)*GH*GH*(1.0-
                     1AA(JMA)*AA(JMA)))
                   24 CONTINUE
                      AX(11,11) = -(2.0*G1)/(GH*GH)
```

```
                AX(11,11) = ((2.0*G1)/(GH*GH))+(G3*EXP(-G2/(THETA(11,N)+1.0)))
                RX(1,1) = (((2.0*GK*G1)/(GH*GH))*X(2,N))+X(1,N)*(1.0-((2.0*GK*G1)/
               1(GH*GH))-(GK*(G3/2.0)*EXP(-G2/(THETA(1,N)+1.0)))))
                DO 19 IMX = 2,10
                XP1 = X(IMX+1,N)*(GK*G1*(GH+2.0*AA(IMX)))/(4.0*AA(IMX)*GH*GH*(1.0-
               1AA(IMX)*AA(IMX))).
                XP2 = X(IMX,N)*(1.0-((GK*G1)/(GH*GH*(1.0-AA(IMX)*AA(IMX)))))-((GK*G
               13*EXP(-G2/(THETA(IMX,N)+1.0)))/(2.0*(1.0-AA(IMX)*AA(IMX))))
                XP3 = X(IMX-1,N)*((GK*G1*(2.0*AA(IMX)-GH))/(4.0*AA(IMX)*GH*GH*(1.0
               1-AA(IMX)*AA(IMX))))
     19         RX(IMX,1) = XP1+XP2+XP3
                RX(11,1) = 0.0
                CALL GELG(RX,AX,11,1,ECUT,IER)
                IN = N+1
                DO 223 IAC = 1,11
                X(IAC,IN) = RX(IAC,1)
    223         FUNC1(IAC) = X(IAC,IN)*(1.0-(AA(IAC)*AA(IAC)))*AA(IAC)
                DO 997 ICS=1,11
                DO 997 KCS=1,11
    997         A(ICS,KCS)=0.0
                A(1,1) = 1.0+((2.0*GK)/(GH*GH))
                A(1,2) = -(2.0*GK)/(GH*GH)
                DO 888 LCS = 2,10
                A(LCS,LCS-1) = (GK*(GH-2.0*AA(LCS)))/(4.0*AA(LCS)*GH*GH*(1.0-AA(LC
               1S)*AA(LCS)))
    888         CONTINUE
                DO 886 MCS = 2,10
                A(MCS,MCS) = 1.0+(GK/(GH*GH*(1.0-AA(MCS)*AA(MCS))))
    886         CONTINUE
                DO 887 NCS=2,10
                A(NCS,NCS+1) = -(GK*(GH+2.0*AA(NCS)))/(4.0*AA(NCS)*GH*GH*(1.0-AA(N
               1CS)*AA(NCS)))
    887         CONTINUE
                A(11,9)=(1.0/15.0)
                A(11,10)=-(16.0/15.0)
                A(11,11)=1.0
                R(1,1) = (((2.0*GK)/(GH*GH))*THETA(2,N))+(THETA(1,N)*(1.0-((2.0*GK
               1)/(GH*GH))))+((GK/2.0)*(X(1,N+1)+X(1,N))*G3*G4*EXP(-G2/(THETA(1,N)
               2+1.0)))
                DO 32 IM = 2,10
                A3 = ((GK*(GH+2.0*AA(IM)))/(4.0*AA(IM)*GH*GH*(1.0-AA(IM)*AA(IM))))
               1*THETA(IM+1,N)
                AC = THETA(IM,N)*(1.0-(GK/(GH*GH*(1.0-AA(IM)*AA(IM)))))
                AD = ((GK*(2.0*AA(IM)-GH))/(4.0*AA(IM)*GH*GH*(1.0-AA(IM)*AA(IM))))
               1*THETA(IM-1,N)
                AE = ((GK*(X(IM,N+1)+X(IM,N))*G3*G4*EXP(-G2/(THETA(IM,N)+1.0)))
               1/(2.0*(1.0-AA(IM)*AA(IM))))
     32         R(IM,1) = AP+AC+AD+AE
                R(11,1)=(2.0/5.0)*GH*GH*X(11,N+1)*G3*G4*EXP(-G2/(THETA(11,N)+1))
                CALL GELG(R,A,11,1,ECUT,IER)
                IN = N+1
                DO 222 IBC=1,11
                THETA(IBC,IN)=R(IBC,1)
    222 FUNC2(IBC)=THETA(IBC,IN)*AA(IBC)*(1.0-AA(IBC)*AA(IBC))
                IF (ICOUNT.LT.6) GO TO 3
                ICOUNT = 1
                DO 51 I=2,10,2
                AREA1 = AREA1 + ((H/3.0)*(FUNC1(I-1)+(4.0*FUNC1(I)) + FUNC1(I+1)))
```

```
                AREA2 = AREA2+((H/3.0)*(FUNC2(I-1)+(4.0*FUNC2(I))+FUNC2(I+1)))
0141
0142          51    CONTINUE
0143                DO 224 IBC=1,11
0144           224  TCEL(IBC,IN)=((THETA(IBC,IN)*TI)+TI-273.15)
0145                WRITE(3,104) IN,IN,IN,IN,IN,IN,(THETA(IABC,IN),TCEL(IABC,IN),X(IAB
                    1C,IN),IABC=1,11)
0146           104  FORMAT(1H1,T2,'VALUES OF THETA(1,',I3,')','TO THETA(11,',I3,')',T4
                    15,'VALUES OF TCEL(1,',I3,')','TO TCEL(11,',I3,')',T86,'VALUES OF X
                    2(1,',I3,')','TO X(11,',I3,')',//(T3,E16.7,T58,F8.4,T92,E16.7
                    3,//))
0147                AVCONS=4.0*AREA1
0148                AVTEMP=4.0*AREA2
0149                WRITE(3,105)AVTEMP,AVCONS
0150          105   FORMAT(//,T2,'AVERAGE TEMPERATURE ',2X,E16.7,T70,'AVERAGE CONCENTR
                    1RATION',E16.7)
0151             3  N = N+1
0152                IF(N.EQ.111) GO TO 630
0153                GO TO 2
0154                END
```